THE SHELL STRUCTURE, MINERALOGY AND RELATIONSHIPS OF THE CHAMACEA (BIVALVIA)

by W. J. KENNEDY, N. J. MORRIS, *and* J. D. TAYLOR

ABSTRACT. The superfamily Chamacea is a group which has constantly confused systematists concerning its relationship with other bivalves. Various authors have related it to the Cardiacea, Veneracea, Crassatellacea, Lucinacea, and the rudists (Hippuritacea).

Most classifications have placed the Chamacea with the rudists; Newell (1965) placing them into the Hippuritoida, a relationship which Yonge (1967) considers beyond doubt. From a review of hard and soft part anatomy, especially shell-structure, dentition, and mineralogy, it seems likely that the Chamacea arose from a group of byssate *Cardita* in the early or middle Cretaceous. Similarities to the rudists are the result of convergent adaptions to a similar mode of life, and there is no real indication of relationship.

The Chamacea should be removed from the order Hippuritoida and placed in the order Veneroida.

THE Chamidae are the sole bivalve family placed in the Superfamily Chamacea (Newell 1965). They are a small group of cemented or secondarily free bivalves which have attracted the attention of zoologists for many years because of the problem of their origins and systematic position. Despite this attention, the systematics of the Recent species is in a very confused state.

Many authors have inferred that the Chamacea are closely related to the rudists (i.e. Odhner 1919, Yonge 1967) and the most recent review of bivalve classification (Newell 1965) places them in the Order Hippuritoida, together with the Megalodontacea and Hippuritacea. We describe the shell structure and mineralogy of recent and fossil Chamidae below, and discuss the use of these features and the nature of the soft part anatomy to determine the natural relationships to other bivalve superfamilies. We have demonstrated elsewhere (Taylor, Kennedy, and Hall 1969) that shell structure and mineralogy are constant features within bivalve superfamilies, and that they are of value in assessing relationships within the Bivalvia.

The Chamacea are characteristic inhabitants of tropical and sub-tropical seas, although some species, such as *Chama pellucida* Broderip, range into cooler temperate waters along the coast of California (San Francisco), but are also present in warmer waters. One species, *Chama gryphina* Lamarck, is present in the Mediterranean.

Chama usually inhabits rocky shores, and is a typical member of the coral reef community. Individuals usually live cemented on rocky surfaces or upon dead coral. Coral-dwelling *Chama* species are usually found on the underside of coral colonies. Most species inhabit the sublittoral and sublittoral fringe environments, but some are intertidal.

Arcinella arcinella (Linnaeus), a Caribbean species, is usually found free living on a coarse gravel substrate (Nicol 1952) but occasionally cemented adults of this species are found. The loss of cementation in *Arcinella* is secondary, for traces of attachment are always to be seen on the juvenile parts of the shell. Certain fossil species such as

[Palaeontology, Vol. 13, Part 3, 1970, pp. 379–413, pl. 70–77.]

Chama calcarata Deshayes from the Calcaire Grossier of the Paris Basin (Eocene, Lutetian), a shell sand facies, also show this secondary loss of cementation.

THE SHELL

1. *General morphology*. The Chamacea are generally inequivalve, asymmetrical, the free valve being the smaller. The lower valve is usually convex and the upper valve is frequently more or less flattened (Pl. 70, fig. 1). Many early Chamacea are rather less inequivalve than extant forms. The secondarily free genus *Arcinella* (Pl. 70, fig. 2) has returned to a more or less equivalve state. The shell of the Chamacea is thick; the umbones are prosogyrous; attachment can be by either valve.

Shell ornament is variable. Some species bear irregular, concentric lamellae, which may be long and foliaceous (Pl. 70, fig. 4); others are spinose, or have irregular, low squamae. Some species have radial ribs as well as concentric lamellae. Ornament varies considerably with environmental conditions such as site of cementation, exposure to wave action and encrusting biota. *Arcinella* is the only genus which consistently bears long spines. Some specimens of *Chama* show a shallow groove running from the umbo to the posterior ventral margin; this is often marked by a supression of strong sculpture. A well-marked, heart-shaped lunule is present in *Arcinella* (Pl. 70, fig. 2).

The interior margin of the shell is frequently crenulate, while the area between the shell edge and the pallial line may be marked by irregular radial grooves and ridges, which are the impressions of the radial masculature of the mantle (Jaworski 1928).

The pallial attachment area (pallial line) is wide, and the dorsal side is overlapped irregularly by inner shell layer. The adductor muscle pads are massive and translucent; they and the pallial line fluoresce blue under ultra-violet light.

2. *Shell geometry*. Growth in the Chamacea has been considered by Yonge (1967) in terms of radial, transverse, and tangential growth components, as discussed by Owen (1953*a*). As they stand, these terms are purely qualitative and have not been mathematically defined. As such they are of limited use in the discussion of shell form.

Lison (1949) described shell coiling in mathematical terms, and more recently Raup (1966) using the same logarithmic spiral, has provided a more comprehensive scheme for the quantitative description of shell coiling. Thus four basic parameters may be used to define the general form of the coiled shell. These are: the shape of the generating curve (S), the whorl expansion rate (W), the distance of the generating curve from the axis (D),

---

EXPLANATION OF PLATE 70

Fig. 1*a*. *Chama macerophylla* Gmelin, Recent, West Indies, cemented to a pebble, ×1. 1*b*, as above, view of right valve, ×1.

Fig. 2. *Arcinella arcinella* (Linnaeus), Recent, West Indies, dorsal view showing lunule, cementation site and prodissoconch (arrow), ×1. 2*a*, as above, lateral view of right valve showing spinose ornament on radial ribs, ×1.

Fig. 3. *Chama pellucida* Broderip, Recent, California, view of inner surface of valve, showing outer translucent calcitic prismatic layer, ×1.

Fig. 4. *Chama frondosa* Broderip, Recent, West America, showing extreme development of frondose squamae, ×1.

Fig. 5. *Gyropleura cenomanensis* d'Orbigny, Cenomanian, Le Mans, France, cemented to valve of *Scabrotrigonia*, ×1·25.

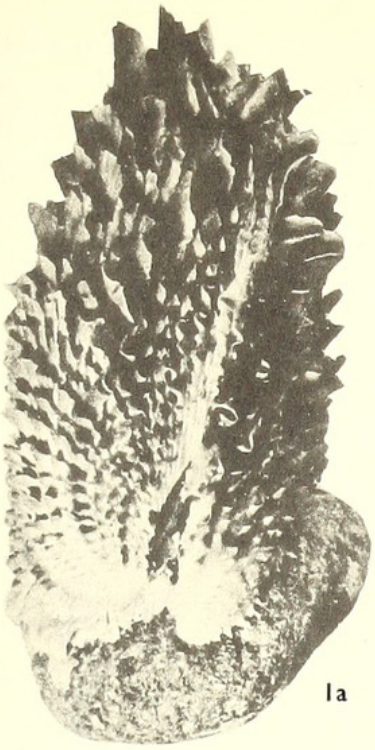

1a

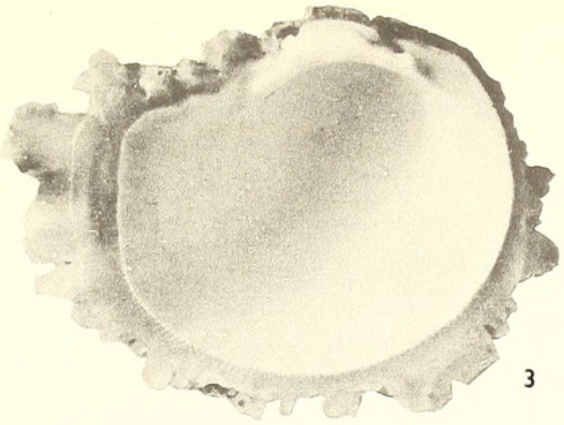

3

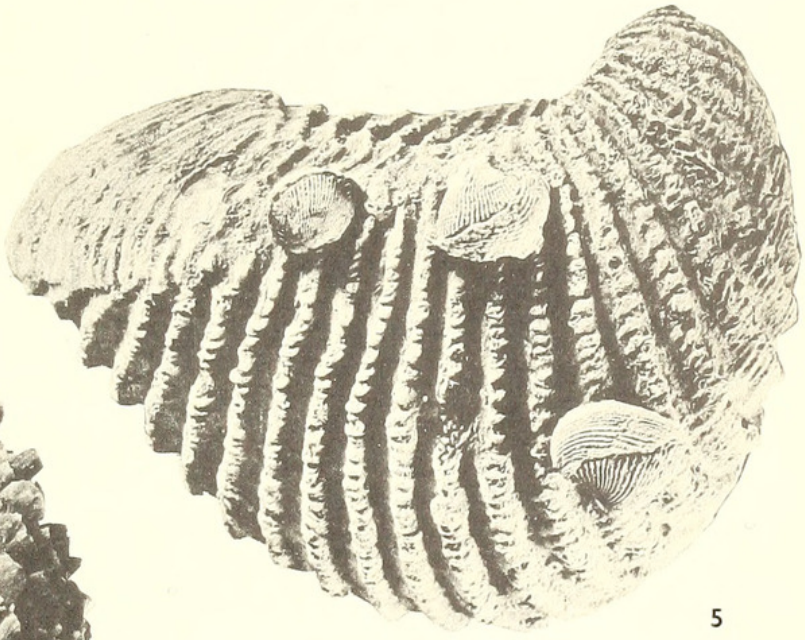

5

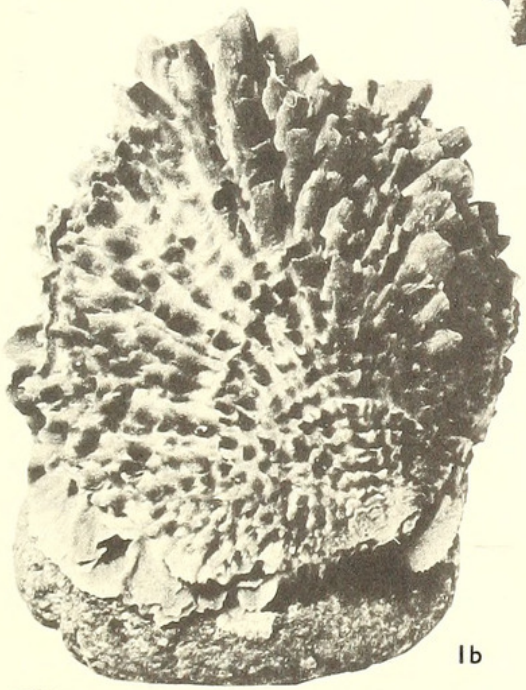

1b

2a

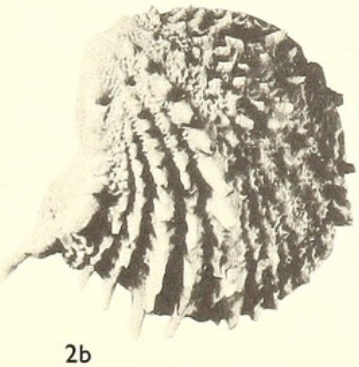

2b

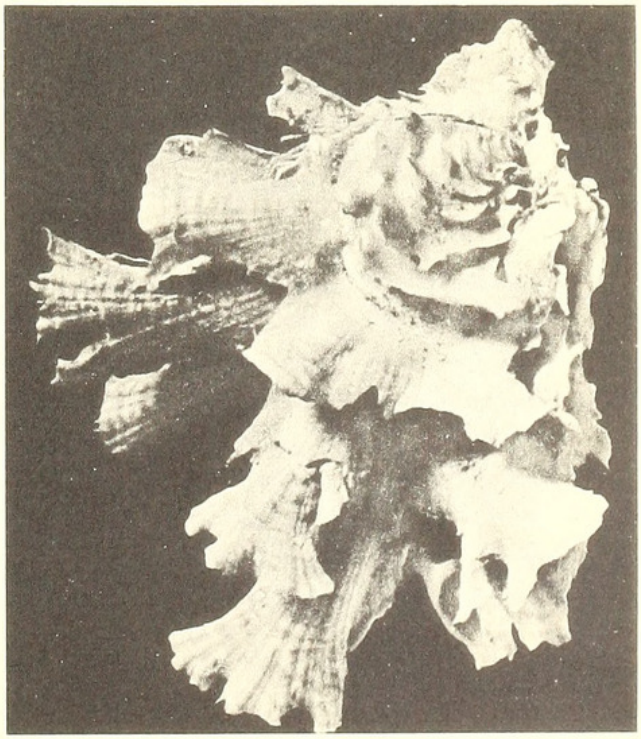

4

KENNEDY, MORRIS and TAYLOR, Chamacea

and the rate of whorl translation parallel to the coiling axis (T) (for full details and derivation see Raup 1966). For most bivalves D is small, and in the Chamacea it is approximately zero. The shape, S, of the generating curve is difficult to define mathematically and is not considered here.

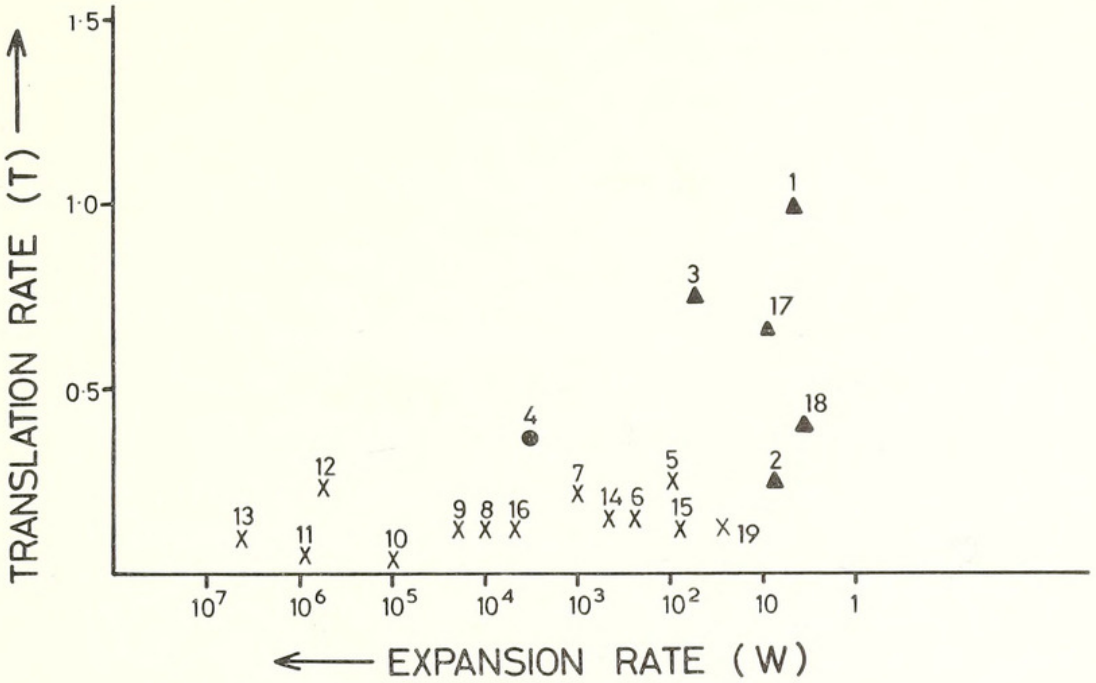

TEXT-FIG. 1. Shell geometry of the Chamacea in relation to other bivalves. Expansion rate (W) plotted against translation rate (T) for a series of uncemented bivalves (X), cemented Chamidae (▲), and the secondarily free *Arcinella arcinella* (●).

Key to numbers:

1, 2. *Chama imbricata* (1 = upper valve, 2 = lower valve).
3. *Chama plicata* Sowerby. Upper valve.
4. *Arcinella arcinella* (Linnaeus). Both valves.
5. *Fragum unedo* (Linnaeus).
6. *Hippopus hippopus* Linnaeus.
7. *Trigonia pectinata* Lamarck.
8. *Codakia tigerina* (Linnaeus).
9. *Mytilus galloprovincialis* Lamarck.
10. *Chlamys varia* Linnaeus.
11. *Gloripecten pallium* (Linnaeus).
12. *Lima squamosa* Lamarck.
13. *Pinctada margaritifera* (Linnaeus).
14. *Crassatella decipiens* Reeve.
15. *Cerastoderma edule* (Linnaeus).
16. *Tellina virgata* (Linnaeus).
17, 18. *Chama gryphina* (Lamarck). (17 = lower valve, 18 = upper valve).
19. *Cardita bicolor* Reeve.

Accurate measurements of W and T are difficult to make in the Chamacea because of the irregular growth form, ornament, and the corroded nature of most shells. Measurements of W and T on *Chama gryphina* Lamarck (text-fig. 1) show that the expansion rate of the lower valve lies between $10^{0.5}$ and $10^{0.9}$, and that of the upper valve is approximately 10. The translation rate of both valves is less than 1. In a specimen of *Chama plicata* Sowerby, where the umbo of the lower valve is strongly enrolled, the translation rate lies between 3·0 and 3·5 whereas that of the upper valve is less than 0·5. Measurements of *Arcinella arcinella* (which has reverted to the uncemented mode of life) show an expansion rate for both valves of approximately $10^{3.5}$. The translation rate is almost zero.

As can be seen from text-fig. 1 the expansion rate of both valves of the cemented Chamacea is low, usually between 10 and 10^2. In 'normal' free-living bivalves such as the Cardiacea and Veneracea, and in *Arcinella*, the expansion rate usually lies between 10^2 and 10^4.

It is clear that the translation rate of any one individual will be variable, according to the substrate upon which original cementation took place. Some repositioning during growth is evident in the attached valve of many individuals, with consequent changes in the translation rate.

3. *The ligament*. The ligament of the Chamacea is opisthodetic, massive, external, but often sunk into a deep groove.

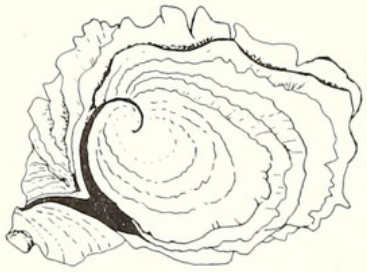

TEXT-FIG. 2. Sketch of *Chama broderipi* Reeve (with strongly enrolled umbos), Recent, Pacific. To show degree of ligament splitting. (Ligament in black.)

The enrolment of the umbonal area causes the ligament to be widely split towards the anterior; each half of the split ligament curls back into the umbones (text-fig. 2).

Three ligament layers are present, an outer thin periostracum, a lamellar layer, and an inner fibrous layer. The outer lamellar layer is thick and wide, and the inner layer is calcified and aragonitic (Pl. 77, fig. 1).

The ligamental splitting is more pronounced than in other bivalves (Stasek 1963 *a*, *b*). Yonge (1967) states that this anterior splitting is due to the rate of growth of the ligament posteriorly exceeding the rate of growth of the valves; this does not seem meaningful as an explanation. The splitting is rather a result of the interumbonal growth produced by the low expansion rate of shell coiling, coupled with a small translation rate. The degree of splitting depends upon the translation rate, which may be rather higher in cemented Chamacea than in the free *Arcinella*. A similar degree of ligamental splitting as is seen in the Chamacea is present in *Glossus* (Owen 1953*b*).

During growth of the shell the ligament elongates in a posteriorward direction. Previously deposited sections of the ligament are overlain by the posteriorward growth of the massive hinge plate.

DEVELOPMENT

The dissoconch stages of Chamacea show a markedly different shell form to that of the adult.

Dissoconchs were examined on very small cemented individuals of *Chama*. Odhner (1919) figured and described some precementation dissoconchs (text-fig. 3, Pl. 71, figs. 1–5). In *Arcinella arcinella* the large dissoconch can frequently be seen preserved at the tips of the umbones on adult shells (Pl. 71, fig. 3).

The first of the shell growth stages is the prodissoconch, formed during the veliger stage. Part of this may be formed by the shell gland rather than the mantle edge. In the Chamacea examined, *Chama pellucida* Broderip, *Chama* sp., and *Arcinella arcinella*, the prodissoconchs (Pl. 71, figs. 1–5) are highly convex, subcircular in outline, translucent, and ornamented only by growth-lines. The form of the prodissoconch indicates a larva either feeding entirely upon the egg yolk during the planktonic stage

(i.e. lecitotrophic), or having direct development and some sort of brood protection (Ockelmann 1962). Yonge (1967) indicates that larval incubation could conceivably occur in *C. pellucida* and *C. exogyra* Conrad.

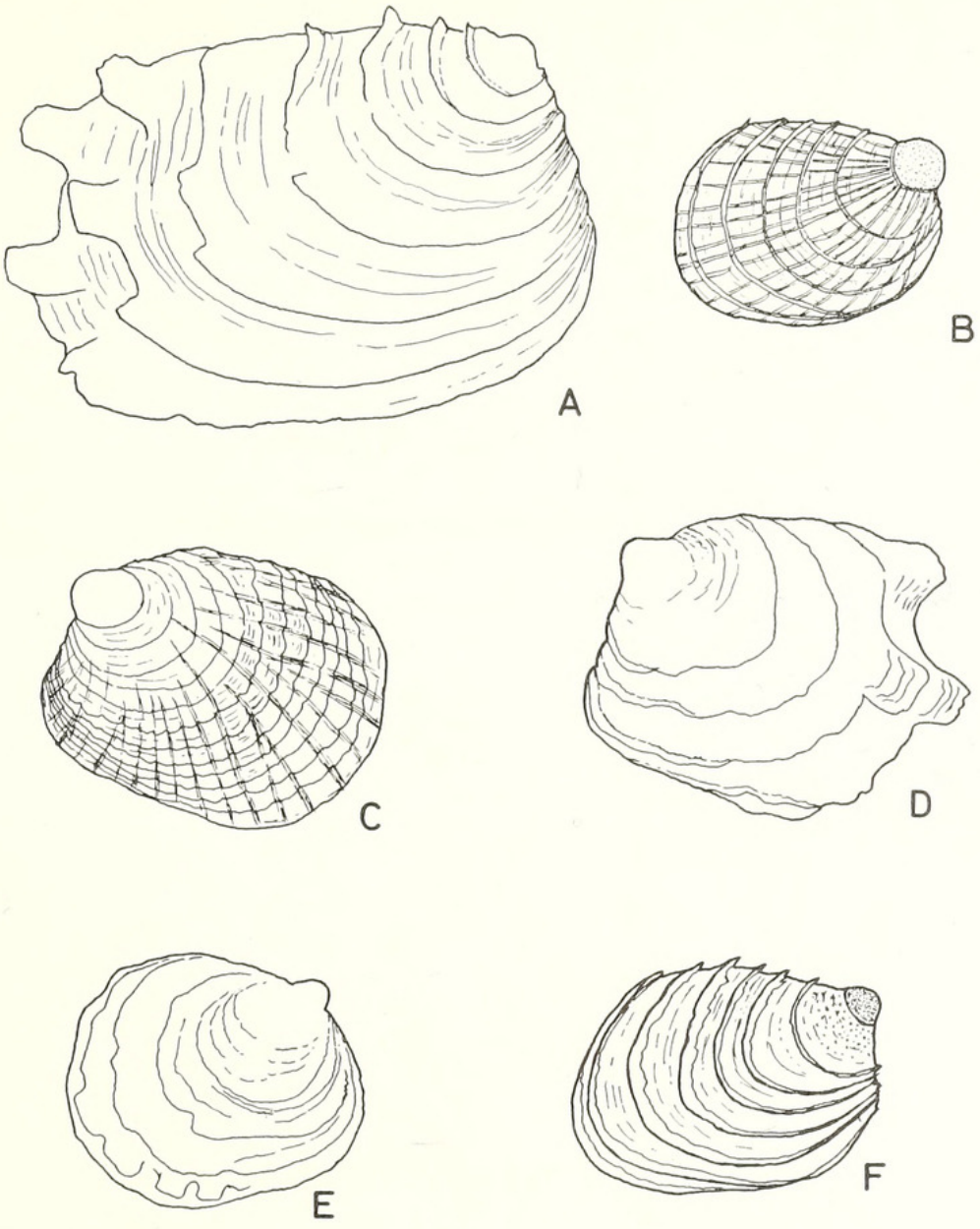

TEXT-FIG. 3. Prodissoconchs and dissoconchs of Recent Chamidae. A. *Arcinella arcinella* (Linnaeus), after Odhner (1919), ×60. B. *Chama pellucida* Broderip, Recent, California, ×60. C. *Chama pusilla* (Odhner), after Odhner (1919), ×40. D, E. *Chama gryphina* Linnaeus, after Odhner (1919), ×60. F. *Chama* sp. East Indies, ×70.

The sharp boundary between prodissoconch and dissoconch (Pl. 71, fig. 2) marks the settlement of the animal on to a substrate. The dissoconch which is secreted by the mantle in the Chamacea is uncemented, equivalve and possesses a sculpture and morphology differing from that of the adult. This stage usually lasts until the young *Chama* is from 0·5 to 1·5 mm. long, but in *Arcinella arcinella* the dissoconch may be prolonged until the individual is 2·5 mm. long. The dissoconch stage is terminated by cementation.

Dissoconch shape is somewhat variable, although a subrectangular or ovate outline is usual (text-fig. 3). Sculpture may consist of thin, widely spaced concentric ribs, as in *Arcinella arcinella* (Pl. 71, fig. 3), in which the outermost parts of the ribs may be projected into small squamae. A similar ornament is seen in *Chama gryphina*.

'*Pseudochama*' *pusilla* Odhner dissoconchs have reticulate ornament (Odhner 1919); *Chama reflexa* Reeve and *C. jukesi* Reeve dissoconchs (Odhner 1919) have radiating ribs. Anthony (1905) figures an unidentified *Chama* dissoconch with fine radiating and concentric ribs. *Chama pellucida* (Pl. 71, fig. 1) has an ornament of fine radiating ribs crossed by about six larger concentric ribs. The early stages of the dissoconch in an unnamed *Chama* show a peculiar pitted ornament (Pl. 71, fig. 5), although the rest of the dissoconch bears concentric ribs only (Pl. 71, fig. 4).

The dentition of the dissoconch is known only from *Arcinella arcinella* (Odhner 1919), *Chama pellucida* (Dall 1903), and an unidentified species (Anthony 1905). In all of these, two cardinals are present in each valve.

An interesting feature of the dissoconch is the subrectangular shape, with a reduced anterior and an elongated posterior portion (text-fig. 3). It is well known that a byssate existence influences the shape of bivalves (Yonge 1962); thus in the Arcacea and some Carditidae a rectangular shape with a long ventral margin is developed. In some *Cardita* species there is a reduction in the anterior part of the animal, which is also seen in the Mytilacea. This purely morphological evidence strongly suggests that the dissoconch stage of some species of *Chama* is byssally attached prior to cementation. The presence of a much larger dissoconch in *Arcinella arcinella* suggests that the byssate existence was prolonged in this species. Unlike most other Chamacea *Arcinella arcinella* inhabits sandy substrates, and the long precementation byssate life may be an insurance against the choice of an unfavourable cementation site.

DENTITION AND INVERSION

Study of the dentition of the Chamacea has given rise to much controversy in the past. The reason for this confusion is that some Chamacea can cement themselves by either the left or the right valve. As a result of attachment by the right valve, the hinge teeth normally present in the left valve appear in the same number and positions in the right valve. As Davis (1935) has pointed out, confusion arises in the interpretation of the teeth of this family by attempting to number teeth in these reversed individuals as though they were in a normal right valve. There are many records of species of *Chama* being attached by either the left valve or the right valve, and even those species which are

---

EXPLANATION OF PLATE 71

Figs. 1, 2. *Chama pellucida* Broderip, Recent, California. 1, Prodissoconch, dissoconch and early adult shell. Note radial and concentric ornament on dissoconch, very different from the squamaceous ornament of the adult. Scanning electron-micrograph, × 140. 2, Detail of the sharp contact between the larval prodissoconch and the dissoconch. Notice close bunching of growth lines as feeding ceases prior to metamorphosis. Scanning electron-micrograph, × 700.

Fig. 3. Prodissoconch and dissoconch of *Arcinella arcinella* Linnaeus, Recent, West Indies showing concentric ornamentation. Scanning electron-micrograph, × 80.

Figs. 4, 5. Prodissoconch and dissoconch of *Chama* sp. from East Indies. 4, Scanning electron-micrograph, × 80. 5, Detail showing the contact between the prodissoconch and the dissoconch, with peculiar pitted ornamentation of the dissoconch. Scanning electron-micrograph, × 340.

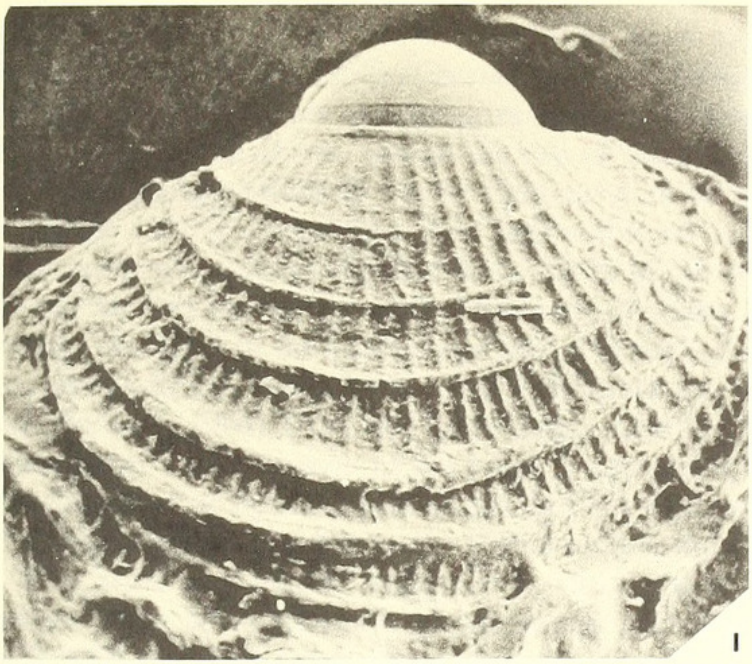

1

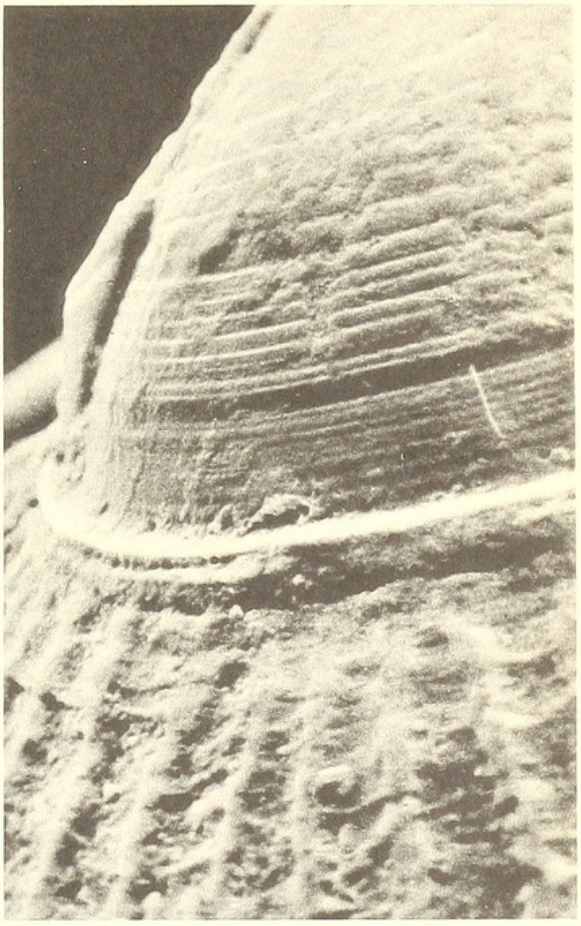

2

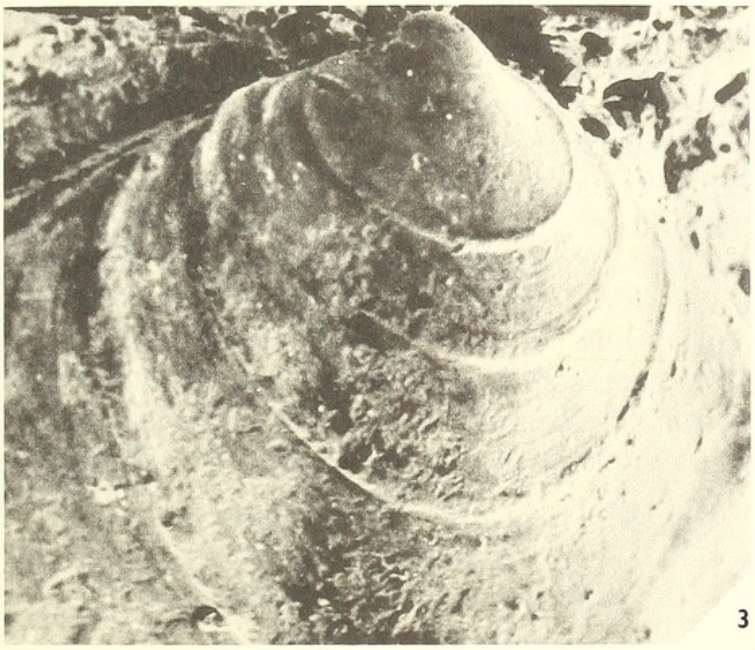

3

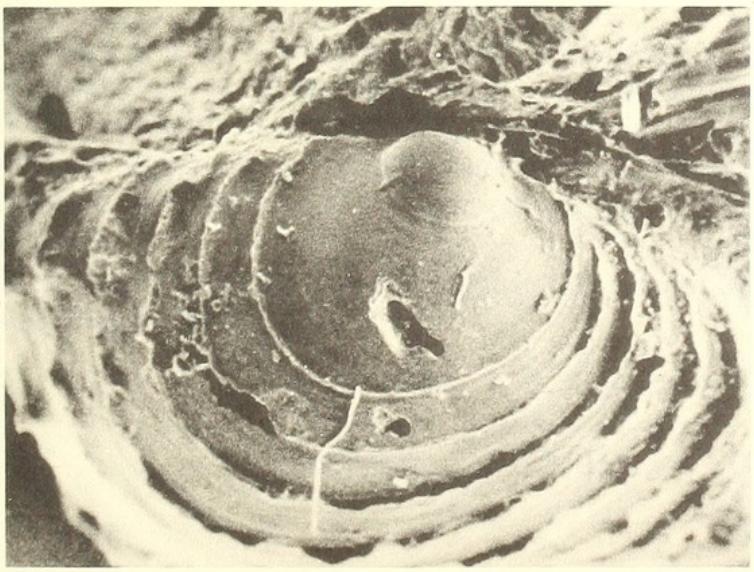

4

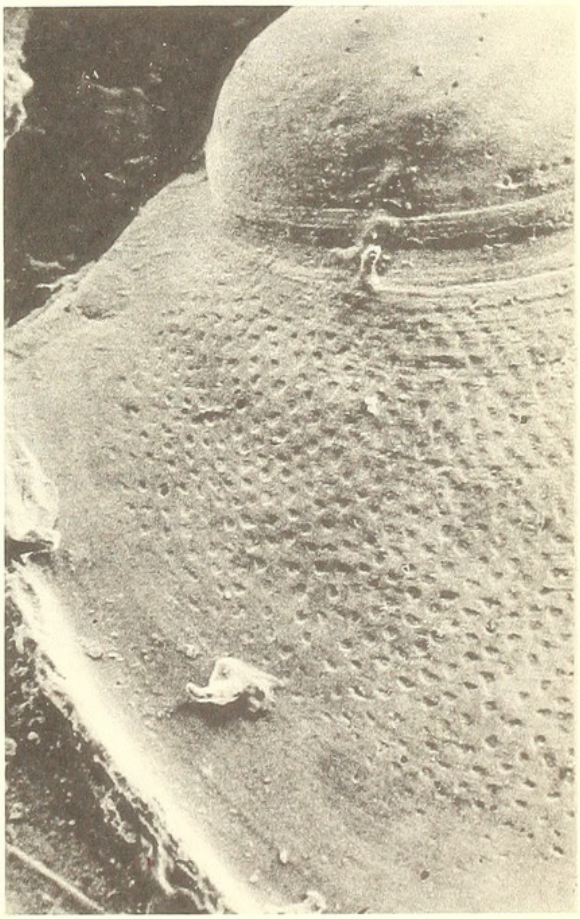

5

KENNEDY, MORRIS and TAYLOR, Chamacea

usually attached by one valve sometimes show attachment by the other (Bayer 1943, Palmer 1928, Yonge 1967). *Chama calcarata* (Eocene, Paris Basin) shows attachment by left and right valves in approximately equal proportions, and this type of variation, plus others noted above, makes the use of the generic name *Pseudochama* Odhner 1919 for those species attached by the right valve of very doubtful validity.

Yonge (1967) stated that it is impossible to homologize the cardinal teeth of the Chamacea with those of other heterodont bivalves because of the great modifications caused by 'tangential growth'. The teeth of many recent species of *Chama* are indeed greatly modified in the adult stage, and it is perhaps easier to study dentition in some of the less modified, fossil forms. The hinge notation used here is that elaborated by Boyd and Newell (1968) from the Steinmann notation, in which every articulating ridge, prominence or depression of the hinge is numbered. This notation system is more objective than that of Bernard (1895) and Munier-Chalmas (1895) which requires knowledge of the ontogenetic development within each family.

The Boyd and Newell system is flexible and is readily convertable to the Bernard system when homologous teeth are recognized. The two valves are illustrated beak to beak with the right valve above the left valve (following Bernard) so that the posterior of the valves lies to the left. The notation is devised to be directly comparable with this. The right valve hinge is expressed by the upper of two lines of symbols and, in both lines, the symbols are arranged from left to right to reflect a traverse along the hinge from the posterior extremity to the anterior extremity. All the structures of the articulating surfaces are indicated. The arabic numeral '1' represents teeth or potentially articular ridges. Inconspicuous or dubious teeth are indicated in brackets. Depressions in the articulating surface which generally function as tooth sockets are indicated as an '0'. Vertical lines, discontinuous in doubtful cases, are used to delimit cardinal from lateral teeth. Various letters such as 'r', 's', 'n', and 'e' are added to represent positions of the resilium, septum, nymph, and elastic ligament, etc.

The basic *Chama* dentition is Bernard's 'lucinoid' type. The hinge notation of *Chama calcarata* (Eocene, Paris Basin) can be expressed as shown below, and in Plate 72, fig. 2:

Right valve	0 1	n (0) (1) 0 1 0 1	
Posterior	———	———————	Anterior.
Left valve	1	n (0) (1) 0 1 0 1 0	

n = ligament nymph

In the left valve the anterior cardinal is large and solid, and the posterior cardinal is long and curved. In the upper right valve, the anterior cardinal is small and ill defined, and the posterior cardinal is long and curved. They are separated by a socket for the reception of the large anterior cardinal of the left valve. Extra articulating ridges are developed between the posterior laterals and the nymphs. They are indicated in parentheses.

This species can be compared with the Recent species *Chama macerophylla* shown below and in Plate 72, fig. 1:

Right valve	0 1 n 0 1 0 1	
Posterior	———————	Anterior.
Left valve	1 (0) n 1 0 1 0	

In the left valve the massive cardinal tooth is very large and grooved. The sockets for the reception of the cardinals of the right valve have fused to form an arcuate socket isolating the cardinal. In the right valve a comparable fusion of the two cardinals has taken place forming a single arcuate tooth. Loss of laterals has also occurred.

In *Arcinella arcinella* (an inverse form) a similar notation occurs, with the fusion of the cardinals and sockets:

Right valve	n 1	0 1 0	
Posterior			Anterior.
Left valve	n 0	1 0 1	

It will be shown below that the dentition of the early Chamacea shows great resemblances to that of the Carditacea.

ANATOMY

Studies on the anatomy of several species of Chamacea have been made by Anthony (1905), Pelseneer (1911), Grieser (1913), Odhner (1919), and most recently by Yonge (1967) who studied *Chama pellucida* and *C. exogyra*. The general anatomical features of the soft parts are summarized below.

The mantle is similar to that of most bivalves, except that the three marginal folds are rather small. The mantle is fused by the inner fold only, to form posteriorly the inhalent and exhalent siphons, and at the anterior to delimit the more extensive pedal gape. The very short siphons represent extensions of the fused inner mantle fold. Yonge (1967) stated that the mantle dorsal to the pedal gape is fused at the inner fold and the inner part of the middle fold. A laterally compressed flap of mantle projects between the valves in the hinge area, forming the mantle isthmus, the termination of which secretes the ligament. The radial musculature of the mantle, which leaves radial markings on the inner shell surface, has been described by Jaworski (1928).

The mantle is attached to the shell by the broad, entire line of pallial muscles, and the adductor muscles. Other, local, points of attachment on the general outer mantle surface are described below. The adductor muscles are large and subequal. The anterior adductor is usually the larger, and curves ventrally to occupy most of the area immediately within the pedal gape.

The foot is small, compressed, and usually pointed. Yonge (1967) considers that the function of the foot is to assist in the cleansing of the mantle cavity, in particular the

---

EXPLANATION OF PLATE 72

Fig. 1. *Chama macerophylla* Gmelin, Recent, Bermuda. BMNH 1911.12.21.1322.3. *a*, Right valve, hinge teeth, ×2. *b*, left valve, ×2. Abbreviations: C, cardinal teeth; L, lateral teeth; n, ligament nymph; add, adductor muscle scar.

Fig. 2. *Chama calcarata* Deshayes, Eocene, Lutetian, Grignon, France. *a*, Right valve, showing hinge teeth, ×2. *b*, Left valve, ×2.

Fig. 3. *Chama* sp. Maastrichtian, Cotentin, France. Silicone rubber cast, ×2.

Fig. 4. *Chama haueri* Zittel, Cretaceous, Senonian Gosau Beds, Gosau, Austria. ×0·75. *b*, dorsal view.

Figs. 5, 6. *Ciplyella pulchra* (Ravn), Cretaceous, Danian, Faxe, Denmark ×1. 5, internal cast, left valve. BMNH L13601. 6, anterior view, BMNH L25558.

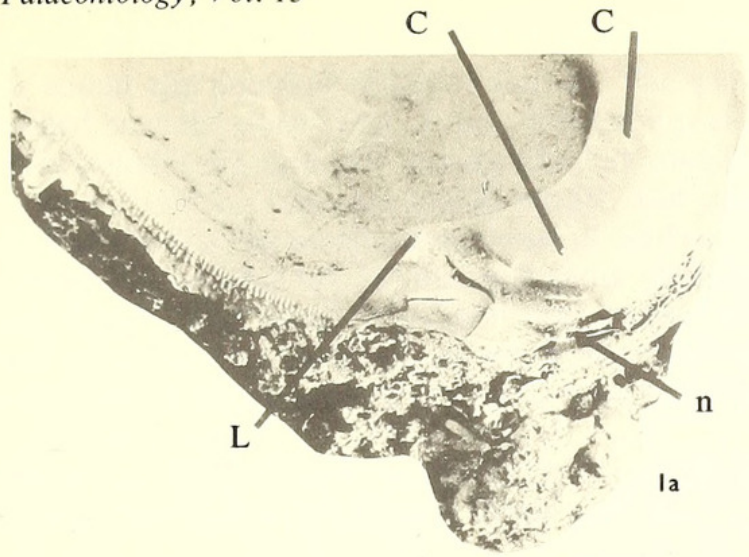

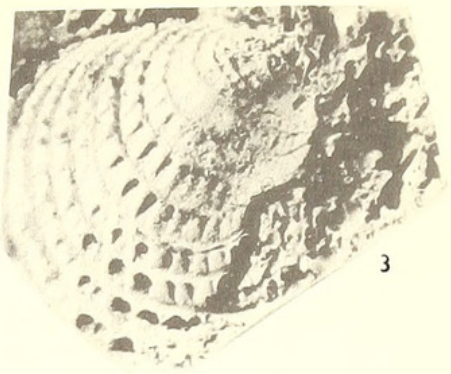

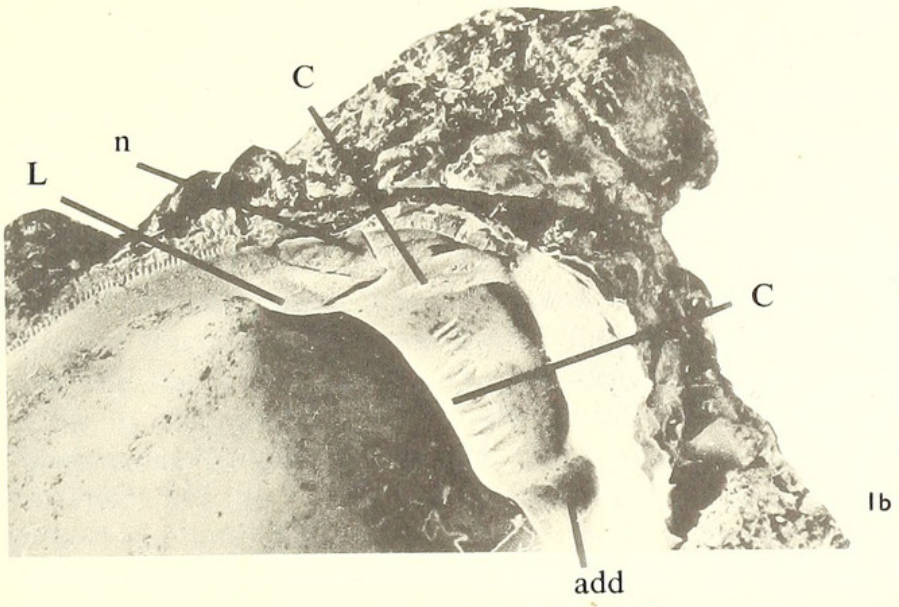

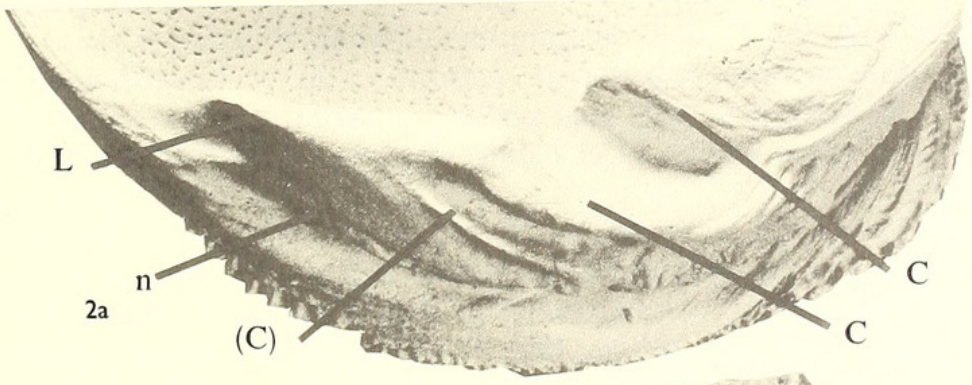

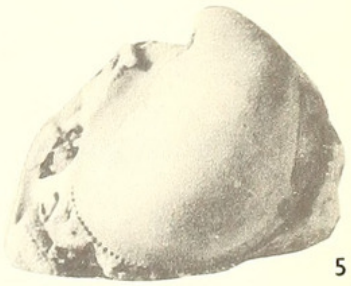

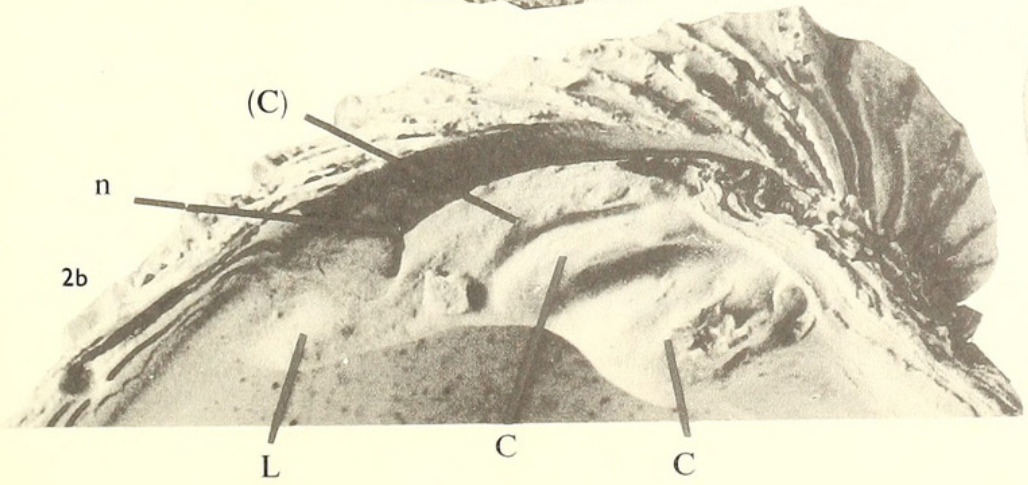

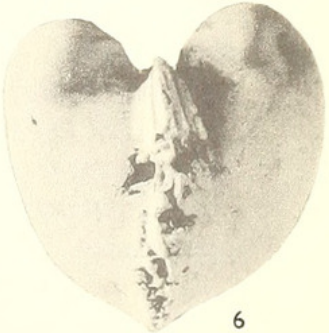

KENNEDY, MORRIS and TAYLOR, Chamacea

area round the anterior adductor muscle. The posterior pedal retractor muscles are attached near the dorsal end of the adductor muscle.

The ctenidia are typically eulamellibranch and have been described in great detail by Odhner (1919). They are highly plicate, and the gill ciliation pattern is type C (1) of Atkins (1937). The labial palps are small, and correspond to type 2 of Stasek (1963*c*), in which the ventral tips of the outermost filaments of the inner demibranches are inserted on to, and fused to, a distal oral groove. The stomach has been discussed by Purchon (1958, 1960) who places the stomach of two species in his types IV and V respectively. A more recent study by Dinamani (1967) places the stomach of *Chama* in his type III*a*.

Other features of the gut, heart, kidneys, nervous and reproductive systems have been described by Grieser (1913) and Odhner (1919).

GEOLOGICAL HISTORY

The generic name *Chama* was used by early workers for many different groups of Cretaceous bivalves, including rudists, *Exogyra*, and other oysters. Pictet and Campiche (1864–7), Stoliczka (1870), and Kutassy (1934) have removed many of these; of the remainder, only five appear to be valid *Chama* species.

Chama coquandi Vidal (1877, 92, pl. 3*a*, fig. 1) is a remarkable Campanian species, in need of reinvestigation. It is inequivalve, but shows no traces of a cementation area, there is no trace of an external ligamental groove or of muscle scars on the internal mould, and the hinge is unknown. The morphology of the valve margin (Vidal 1877, pl. 4, fig. 6) is comparable to that seen in other *Chama* species.

Chama haueri Zittel (1865, 147, pl. 7, figs. 3 *a–c*; see herein Pl. 72, fig. 4) and *C. detrita* Zittel (1865, 147, pl. 7, figs. 4 *a–b*) from the Gosau Beds, Austria, of Senonian age; *C. callosa* Noetling (1902, 50, pl. 12, figs. 9–10) from the Upper Cretaceous of Baluchistan; and *C. toeroeki* Pethö (1906, 269, pl. 19, figs. 15–16) from the Upper Cretaceous of Hungary are all good *Chama* species.

C. haueri is based on material retaining the shell, *C. detrita* on internal moulds. From our knowledge of variation in other species, these are probably synonyms, the trivial name *haueri* taking priority. *C. callosa* may also be a synonym.

All these Cretaceous forms are similar in having an ornament of concentric lamellae (Pl. 72, figs. 3, 4).

Douvillé (1913, 453) also records Chamidae from the Upper Cretaceous of France, but from horizons above that of the Gosau material. We have also seen an undescribed form from the Calcaire à baculites (Maastrichtian) of Cotentin, France (Pl. 72, fig. 3).

Chama angulosa d'Orbigny (1844, 690, pl. 464, figs. 8–9), *Chama gasoli* Vidal (1877, 93, pl. 4, figs. 7 *a–b*), and *C. moritzi* Strombeck (1863, 156) are all species of *Gyropleura*. *C. spondyloides* Bayle (1856, 365, pl. 14, fig. 1) is a monopleurid rudist. *C. triedra* Pictet and Campiche (1867, 5, pl. 140, figs. 4–5) and *C. gracilicornis* Pictet and Campiche (1867, 6, pl. 140, figs. 6–7) are both diceratid rudists. *C. boulei* Basse (1933, 43, pl. 7, fig. 6) is probably a *Spondylus*. *C. deplanata* Stoliczka (1870, 235, pl. 22, fig. 5) is probably a *Plicatula*. *C. bifrons* Griepenkerl (1899, 362, pl. 7, fig. 2), *C. costata* Roemer (1841, 67, pl. 8, fig. 20), *C. multicostata* Wegner (1905, 192, text-fig. 19), and *C. geometrica* Roemer (1840, 35, pl. 18, fig. 39) are all oysters.

Chama cretacea d'Orbigny (1846, 689, pl. 463, figs. 1–2) is generically indeterminate, but does not seem to be a *Chama*. *Chama suborbiculata* d'Orbigny (1822, 100), is not figured, whilst d'Orbigny's description is brief. It may be a *Chama*, but is best regarded as a *nomen dubium* until re-studied.

Little is known of *Chama* in Danian, Montian or Thanetian rocks. *Ciplyella pulchra* (Ravn) (1902, 127, pl. 4, figs. 12–15) from the Danian Koralkalk of Denmark seems to belong to the Monopleuridae (see p. 409). *Chama ciplyensis* Vincent (1928, 104, pl. 5, fig. 17) from the Danian or Montian Poudingue de Ciply of Belgium is little known. The description of its adductor scars suggest that it is a genuine *Chama*. *Chama ancestralis* Cossmann (1908, 44, pl. 1, figs. 38–40) from the Montian Calcaire Grossier of Belgium is known from two specimens only and needs reinvestigation.

In the Eocene *Chama* becomes much more common, being represented by such familiar forms as *Chama squamosa*, *C. lamellosa*, and *C. gigas*.

Arcinella (type species *Chama arcinella* Linnaeus) is a tropical American chamid which appears in the early Miocene of the Florida region. It is thought to be derived from the early to middle Miocene species *Chama draconis* Dall (Nicol 1952).

Most of the fossil occurrences of *Chama* are in association with rich shallow marine faunas of tropical or subtropical aspect.

C. exogyra and *C. pellucida* occur associated with cooler water faunas, as do living members of the same species.

SHELL STRUCTURE AND MINERALOGY

Shells of more than thirty species of recent and fossil Chamidae were examined in connection with this work.

Mineralogical determinations were carried out by means of standard X-ray diffraction techniques. Optical examinations of shell structure were made on shell interiors, fractured sections, acetate peels of polished and etched sections (method in Kummel and Raup 1965), and petrographic thin sections.

Fine structure was studied on surfaces, fractured and polished and etched sections, which were examined with a Cambridge Instrument Company 'Stereoscan' scanning electron microscope.

The shell of most species examined is wholly aragonitic, with a two-layered shell. Exceptions are *Chama pellucida* and *Chama exogyra* which have an additional outer prismatic calcite layer. The significance of this is discussed below.

The results of our observations are summarized in Table 1. It will be seen that we use the terms inner, middle, and outer shell layers. This is an entirely topographic, and thus unambiguous division. We reject Oberling's (1964) use of the terms ectostracum, mesostracum, and endostracum for three-layered shells, mesectostracum and mesendostracum for two-layered shells as this implies homology between layers in different shells. It further suggests that two-layered shells may be derived from three-layered forms.

As well as speaking of shell layers, we have adopted Oberling's (1964) term *myostracum* for the peculiar blocky prismatic aragonite laid down under sites of muscle attachment, i.e. the pallial, pedal, and adductor myostraca.

(*a*) *Structure of the crossed-lamellar layer.* Crossed-lamellar structure forms the outer shell layer of most species (text-fig. 4), but the middle layer of *Chama pellucida* and *C. exogyra* (text-fig. 5).

Conventional microscopy shows the inner surface of the shell layer as a series of elongate, branching, interdigitating lenses. These lenses are arranged with their long axes running concentrically, i.e. essentially parallel to the shell margin over most of the shell.

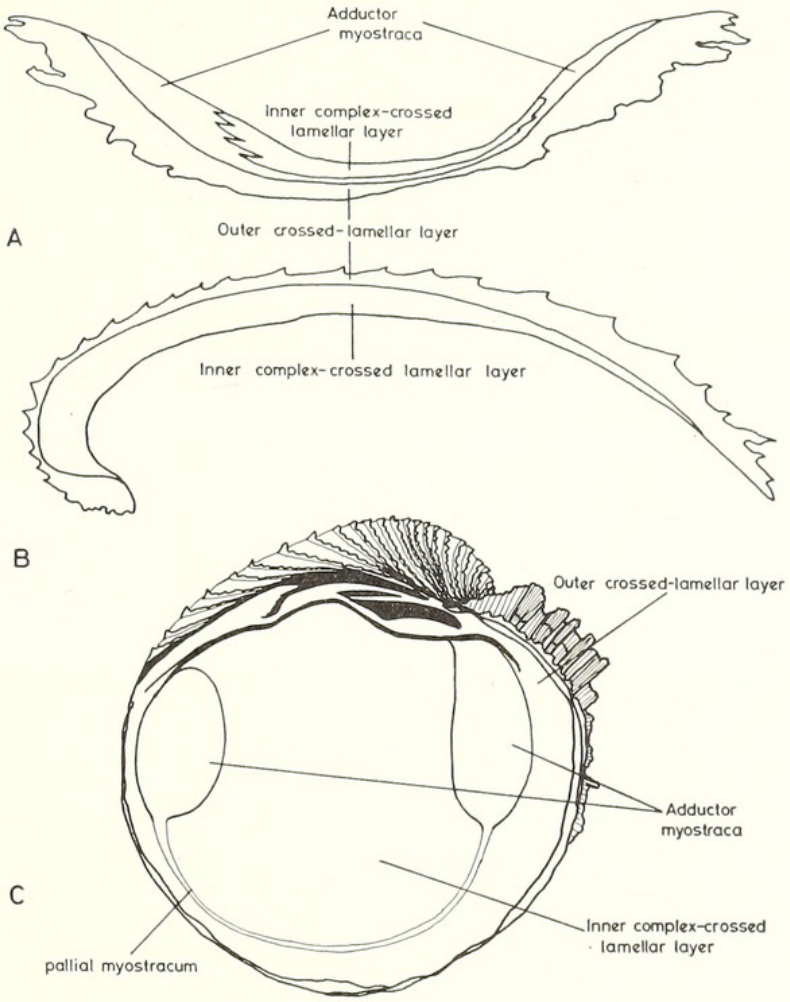

TEXT-FIG. 4. (A) Transverse section, (B) longitudinal section, and (C) interior of *Chama macerophylla* Gmelin to show distribution of shell layers.

More variable orientations are developed on spines, squamae, and in the umbonal region. These lenses correspond to the outcrop of the first order lamels of Bøggild (1930).

In section first-order lamels run normal to the inner surface of the shell layer (Pl. 73, fig. 1). Traced towards the shell exterior they twist and turn however, producing complicated patterns. The first-order lamels branch and interdigitate in sections in much the same way as they do on shell interiors. A strong, interlocking structure is thus produced.

First-order lamels are up to several millimetres long and of the order of 0·5 mm. thick. Sections and peels show a striking colour banding, adjacent lamels being straw-yellow or red-brown in colour.

Within each first-order lamel (text-fig. 6*b*) there are sheet-like second-order lamels (Bøggild 1930). These are in turn built of minute laths, about 1 μ in diameter and some

TABLE 1. Shell structure and mineralogy of recent and fossil Chamacea

Species	*Horizon and locality*	*Mineralogy*	*Outer layer*	*Inner layer*	*Myostraca* *Pallial*	*Adductor*	*Observations*
Chama haueri Zittel	Senonian, Gosau, Austria	Aragonite	Crossed-lamellar	Complex crossed-lamellar with sheets of myostracal-type prisms	Prismatic	Prismatic	
Chama calcarata Lamarck	Lutetian, Chaumont en Vexin, France		Crossed-lamellar	Complex crossed-lamellar with sheets of myostracal-type prisms	Prismatic	Prismatic	
Chama calcarata Lamarck	Lutetian, Mouchy, France		Crossed-lamellar	Complex crossed-lamellar with sheets of myostracal-type prisms	Prismatic	Prismatic	Myostracal sheets in inner layer locally folded (see text)
Chama lamellosa Lamarck	Lutetian, Damercy, France	Aragonite	Crossed-lamellar	Complex crossed-lamellar with sheets of myostracal-type prisms	Prismatic	Prismatic	
Chama gigas Deshayes	Lutetian, Grignon, France		Crossed-lamellar	Complex crossed-lamellar with sheets of myostracal-type prisms	Prismatic	Prismatic	Myostracal sheets in inner layer similar to those in *C. calcarata*
Chama selseiensis S. V. Wood	Lutetian, Brackle-sham, England		Crossed-lamellar	Complex crossed-lamellar with sheets of myostracal-type prisms and myostracal pillars	Prismatic	Prismatic	
Chama turgida Lamarck	Basal Auversian, Chavençon, France		Crossed-lamellar	Complex crossed-lamellar with sheets of myostracal-type prisms and myostracal pillars	Prismatic	Prismatic	Scattered tubules in inner layer
Chama fimbriata Defrance	Auversian, Auvers, France		Crossed-lamellar	Complex crossed-lamellar with sheets of myostracal-type prisms	Prismatic	Prismatic	
Chama papyracea Deshayes	Auversian, Auvers, France		Crossed-lamellar	Complex crossed-lamellar with sheets of myostracal-type prisms	Prismatic	Prismatic	
Chama squamosa Solander	Bartonian, Barton, England		Crossed-lamellar	Complex crossed-lamellar with sheets of myostracal-type prisms	Prismatic	Prismatic	Scattered tubules in inner layer
Chama squamosa Solander	Ludian, Chavanion, France		Crossed-lamellar	Complex crossed-lamellar with sheets of myostracal-type prisms and myostracal pillars	Prismatic	Prismatic	Scattered tubules in inner layer

Chama aquitanica Cossman and Pissarro	Aquitanian, Villandrani, Italy	Crossed-lamellar	Complex crossed-lamellar with sheets of myostracal-type prisms	Prismatic	Prismatic	
Chama sp.	Miocene, San Domingo	Crossed-lamellar	Complex crossed-lamellar with sheets of myostracal-type prisms	Prismatic	Prismatic	
Chama crassa Chenu	Pliocene, Florida	Crossed-lamellar	Complex crossed-lamellar with thin sheets of myostracal-type prisms	Prismatic	Prismatic	Scattered tubules in inner layer
Chama heilprini (Nicol)	Plio-Pleistocene, La Belle, Florida	Crossed-lamellar	Complex crossed-lamellar with sheets of myostracal-type prisms and myostracal pillars	Prismatic	Prismatic	Scattered tubules in inner layer
Chama brocchii Deshayes	Pleistocene, Astigiana, Italy	Crossed-lamellar	Complex crossed-lamellar with sheets of myostracal-type prisms	Prismatic	Prismatic	Scattered tubules in inner layer
Chama gryphina Lamarck	Pleistocene, Piedmont, Italy	Crossed-lamellar	Complex crossed-lamellar with sheets of myostracal-type prisms	Prismatic	Prismatic	
Chama gryphina Lamarck	Pleistocene, Astigiana, Italy	Crossed-lamellar	Complex crossed-lamellar with thin sheets of myostracal-type prisms	Prismatic	Prismatic	
Chama nivalis Reeve	Pleistocene, Berbera, Somalia	Crossed-lamellar with scattered myostracal pillars	Complex crossed-lamellar with sheets of myostracal-type prisms and myostracal pillars	Prismatic	Prismatic	Myostracal pillars in the inner parts of the outer layer; scattered myostracal pillars in inner layer. Tubules in inner layer
Chama pulchella Reeve	Pleistocene, Berbera, Somalia	Crossed-lamellar	Complex crossed-lamellar with sheets of myostracal-type prisms and myostracal pillars	Prismatic	Prismatic	Tubules in inner layer
Arcinella arcinella antiquata (Dall)	Miocene, Colombia	Crossed-lamellar	Complex crossed-lamellar with sheets of myostracal-type prisms	Prismatic	Prismatic	
Arcinella trachyderma (Pilsbry and Johnson)	Miocene, San Domingo	Crossed-lamellar	Complex crossed-lamellar with sheets of myostracal-type prisms	Prismatic	Prismatic	

TABLE 1. Shell structure and mineralogy of recent and fossil Chamacea

Species	*Horizon and locality*	*Mineralogy*	*Outer layer*	*Inner layer*	*Myostraca* *Pallial*	*Adductor*	*Observations*
Chama haueri Zittel	Senonian, Gosau, Austria	Aragonite	Crossed-lamellar	Complex crossed-lamellar with sheets of myostracal-type prisms	Prismatic	Prismatic	
Chama calcarata Lamarck	Lutetian, Chaumont en Vexin, France		Crossed-lamellar	Complex crossed-lamellar with sheets of myostracal-type prisms	Prismatic	Prismatic	
Chama calcarata Lamarck	Lutetian, Mouchy, France		Crossed-lamellar	Complex crossed-lamellar with sheets of myostracal-type prisms	Prismatic	Prismatic	Myostracal sheets in inner layer locally folded (see text)
Chama lamellosa Lamarck	Lutetian, Damercy, France	Aragonite	Crossed-lamellar	Complex crossed-lamellar with sheets of myostracal-type prisms	Prismatic	Prismatic	
Chama gigas Deshayes	Lutetian, Grignon, France		Crossed-lamellar	Complex crossed-lamellar with sheets of myostracal-type prisms	Prismatic	Prismatic	Myostracal sheets in inner layer similar to those in *C. calcarata*
Chama selseiensis S. V. Wood	Lutetian, Brackle-sham, England		Crossed-lamellar	Complex crossed-lamellar with sheets of myostracal-type prisms and myostracal pillars	Prismatic	Prismatic	
Chama turgida Lamarck	Basal Auversian, Chavençon, France		Crossed-lamellar	Complex crossed-lamellar with sheets of myostracal-type prisms and myostracal pillars	Prismatic	Prismatic	Scattered tubules in inner layer
Chama fimbriata Defrance	Auversian, Auvers, France		Crossed-lamellar	Complex crossed-lamellar with sheets of myostracal-type prisms	Prismatic	Prismatic	
Chama papyracea Deshayes	Auversian, Auvers, France		Crossed-lamellar	Complex crossed-lamellar with sheets of myostracal-type prisms	Prismatic	Prismatic	
Chama squamosa Solander	Bartonian, Barton, England		Crossed-lamellar	Complex crossed-lamellar with sheets of myostracal-type prisms	Prismatic	Prismatic	Scattered tubules in inner layer
Chama squamosa Solander	Ludian, Chavanion, France		Crossed-lamellar	Complex crossed-lamellar with sheets of myostracal-type prisms and myostracal pillars	Prismatic	Prismatic	Scattered tubules in inner layer
Chama aquitanica Cossman and Pissarro	Aquitanian, Villandrani, Italy		Crossed-lamellar	Complex crossed-lamellar with sheets of myostracal-type prisms	Prismatic	Prismatic	
Chama sp.	Miocene, San Domingo		Crossed-lamellar	Complex crossed-lamellar with sheets of myostracal-type prisms	Prismatic	Prismatic	
Chama crassa Chenu	Pliocene, Florida		Crossed-lamellar	Complex crossed-lamellar with thin sheets of myostracal-type prisms	Prismatic	Prismatic	Scattered tubules in inner layer
Chama heilprini (Nicol)	Plio-Pleistocene, La Belle, Florida		Crossed-lamellar	Complex crossed-lamellar with sheets of myostracal-type prisms and myostracal pillars	Prismatic	Prismatic	Scattered tubules in inner layer
Chama brocchii Deshayes	Pleistocene, Asti-giana, Italy		Crossed-lamellar	Complex crossed-lamellar with sheets of myostracal-type prisms	Prismatic	Prismatic	Scattered tubules in inner layer
Chama gryphina Lamarck	Pleistocene, Pied-mont, Italy		Crossed-lamellar	Complex crossed-lamellar with sheets of myostracal-type prisms	Prismatic	Prismatic	
Chama gryphina Lamarck	Pleistocene, Asti-giana, Italy		Crossed-lamellar	Complex crossed-lamellar with thin sheets of myostracal-type prisms	Prismatic	Prismatic	
Chama nivalis Reeve	Pleistocene, Berbera, Somalia		Crossed-lamellar with scattered myostracal pillars	Complex crossed-lamellar with sheets of myostracal-type prisms and myostracal pillars	Prismatic	Prismatic	Myostracal pillars in the inner parts of the outer layer; scattered myo-stracal pillars in inner layer. Tubules in inner layer
Chama pulchella Reeve	Pleistocene, Berbera, Somalia		Crossed-lamellar	Complex crossed-lamellar with sheets of myostracal-type prisms and myostracal pillars	Prismatic	Prismatic	Tubules in inner layer
Arcinella arcinella antiquata (Dall)	Miocene, Colombia		Crossed-lamellar	Complex crossed-lamellar with sheets of myostracal-type prisms	Prismatic	Prismatic	
Arcinella trachyderma (Pilsbry and Johnson)	Miocene, San Domingo		Crossed-lamellar	Complex crossed-lamellar with sheets of myostracal-type prisms	Prismatic	Prismatic	

Specie	*Horizon and locality*	*Mineralogy*	*Outer layer*	*Inner layer*	*Myostraca* *Pallial*	*Adductor*	*Observations*
Arcinella arcinella arcinella (Linnaeus)	Pliocene, Caloosahatchee, Florida		Crossed-lamellar	Complex crossed-lamellar with sheets of myostracal-type prisms	Prismatic	Prismatic	
Arcinella arcinella (Linnaeus)	W. Florida	Aragonite	Crossed-lamellar	Complex crossed-lamellar	Thin prismatic	Thick prismatic	Layers of myostracal-type prisms present in inner layer; other specimens have myostracal pillared tubules
Chama aspera Reeve	Indian Ocean	Aragonite	Crossed-lamellar	Complex crossed-lamellar	Thin prismatic	Thick prismatic	Myostracal pillars in inner layer
Chama brassica Reeve	Philippines	Aragonite	Crossed-lamellar	Complex crossed-lamellar	Thin prismatic	Thick prismatic	Thin bands of myostracal-type prisms and tubules in the inner layer
Chama gryphina Lamarck	Mediterranean	Aragonite	Crossed-lamellar	Complex crossed-lamellar	Thin prismatic	Thick prismatic	Myostracal pillars and scattered tubules in inner layer; some specimens have bands of myostracal-type prisms in this layer
Chama iostoma Reeve	Aden	Aragonite	Crossed-lamellar	Complex crossed-lamellar	Thin prismatic	Thick prismatic	Abundant myostracal pillars and scattered pillars in inner layer. Other (? pedal) myostraca in some sections
Chama lazarus Wood	Mombasa, E. Africa	Aragonite	Crossed-lamellar	Complex crossed-lamellar	Thin prismatic	Thick prismatic	Abundant myostracal pillars and scattered tubules in the inner layer. Tubules may be present in the marginal parts of the outer layer. The internal ligament is aragonitic
Chama nubea Reeve	Philippines	Aragonite	Crossed-lamellar	Complex crossed-lamellar	Thin prismatic	Thick prismatic	Abundant radially elongate myostracal pillars and scattered tubules in the inner layer

Chama sarda Reeve	W. Indies	Aragonite	Crossed-lamellar	Complex crossed-lamellar	Thin prismatic	Thick prismatic	Myostracal pillars and scattered tubules in the inner layer
Chama spinosa Broderip	Dunken Island, Cape York, Queensland	Aragonite	Crossed-lamellar	Complex crossed-lamellar	Thin prismatic	Thick prismatic	Tubules present in the inner layer; myostracal pillars occur in some specimens
Chama spondylodes Menke	Queensland	Aragonite	Crossed-lamellar	Complex crossed-lamellar	Thin prismatic	Thick prismatic	Tubules, sheets of myostracal-type prisms and myostracal pillars are present in the inner layer; the latter extend into the outer layer
Chama macerophylla Gmelin	W. Indies	Aragonite	Crossed-lamellar	Complex crossed-lamellar	Thin prismatic	Thick prismatic	Myostracal pillars and abundant tubules in the inner layer
Chama corrugata Broderip	Ecuador	Aragonite	Crossed-lamellar	Complex crossed-lamellar	Thin prismatic	Thick prismatic	The inner layer has a rather coarse fabric, and myostracal pillars in the umbonal area
Chama radians Lamarck	W. Indies	Aragonite	Crossed-lamellar	Complex crossed-lamellar	Thin prismatic	Thick prismatic	Abundant myostracal pillars in the inner layer

				Middle layer	*Inner layer*	*Myostraca*	
						Pallial	*Adductor*
Chama pellucida Broderip	California	Aragonite and Calcite	Granular/prismatic calcite	Crossed-lamellar aragonite	Complex crossed-lamellar aragonite	Thin prismatic aragonite	Thin prismatic aragonite

Specie	Horizon and locality	Mineralogy	Outer layer	Inner layer	Myostraca: Pallial	Myostraca: Adductor	Observations
Arcinella arcinella arcinella (Linnaeus)	Pliocene, Caloosahatchee, Florida		Crossed-lamellar	Complex crossed-lamellar with sheets of myostracal-type prisms	Prismatic	Prismatic	
Arcinella arcinella (Linnaeus)	W. Florida	Aragonite	Crossed-lamellar	Complex crossed-lamellar	Thin prismatic	Thick prismatic	Layers of myostracal-type prisms present in inner layer; other specimens have myostracal pillared tubules
Chama aspera Reeve	Indian Ocean	Aragonite	Crossed-lamellar	Complex crossed-lamellar	Thin prismatic	Thick prismatic	Myostracal pillars in inner layer
Chama brassica Reeve	Philippines	Aragonite	Crossed-lamellar	Complex crossed-lamellar	Thin prismatic	Thick prismatic	Thin bands of myostracal-type prisms and tubules in the inner layer
Chama gryphina Lamarck	Mediterranean	Aragonite	Crossed-lamellar	Complex crossed-lamellar	Thin prismatic	Thick prismatic	Myostracal pillars and scattered tubules in inner layer; some specimens have bands of myostracal-type prisms in this layer
Chama iostoma Reeve	Aden	Aragonite	Crossed-lamellar	Complex crossed-lamellar	Thin prismatic	Thick prismatic	Abundant myostracal pillars and scattered pillars in inner layer. Other (? pedal) myostraca in some sections
Chama lazarus Wood	Mombasa, E. Africa	Aragonite	Crossed-lamellar	Complex crossed-lamellar	Thin prismatic	Thick prismatic	Abundant myostracal pillars and scattered tubules in the inner layer. Tubules may be present in the marginal parts of the outer layer. The internal ligament is aragonitic
Chama nubea Reeve	Philippines	Aragonite	Crossed-lamellar	Complex crossed-lamellar	Thin prismatic	Thick prismatic	Abundant radially elongate myostracal pillars and scattered tubules in the inner layer

Chama sarda Reeve	W. Indies	Aragonite	Crossed-lamellar	Complex crossed-lamellar	Thin prismatic	Thick prismatic	Myostracal pillars and scattered tubules in the inner layer
Chama spinosa Broderip	Dunken Island, Cape York, Queensland	Aragonite	Crossed-lamellar	Complex crossed-lamellar	Thin prismatic	Thick prismatic	Tubules present in the inner layer; myostracal pillars occur in some specimens
Chama spondylodes Menke	Queensland	Aragonite	Crossed-lamellar	Complex crossed-lamellar	Thin prismatic	Thick prismatic	Tubules, sheets of myostracal-type prisms and myostracal pillars are present in the inner layer; the latter extend into the outer layer
Chama macerophylla Gmelin	W. Indies	Aragonite	Crossed-lamellar	Complex crossed-lamellar	Thin prismatic	Thick prismatic	Myostracal pillars and abundant tubules in the inner layer
Chama corrugata Broderip	Ecuador	Aragonite	Crossed-lamellar	Complex crossed-lamellar	Thin prismatic	Thick prismatic	The inner layer has a rather coarse fabric, and myostracal pillars in the umbonal area
Chama radians Lamarck	W. Indies	Aragonite	Crossed-lamellar	Complex crossed-lamellar	Thin prismatic	Thick prismatic	Abundant myostracal pillars in the inner layer

				Middle layer	Inner layer	Myostraca: Pallial	Myostraca: Adductor
Chama pellucida Broderip	California	Aragonite and Calcite	Granular/prismatic calcite	Crossed-lamellar aragonite	Complex crossed-lamellar aragonite	Thin prismatic aragonite	Thin prismatic aragonite

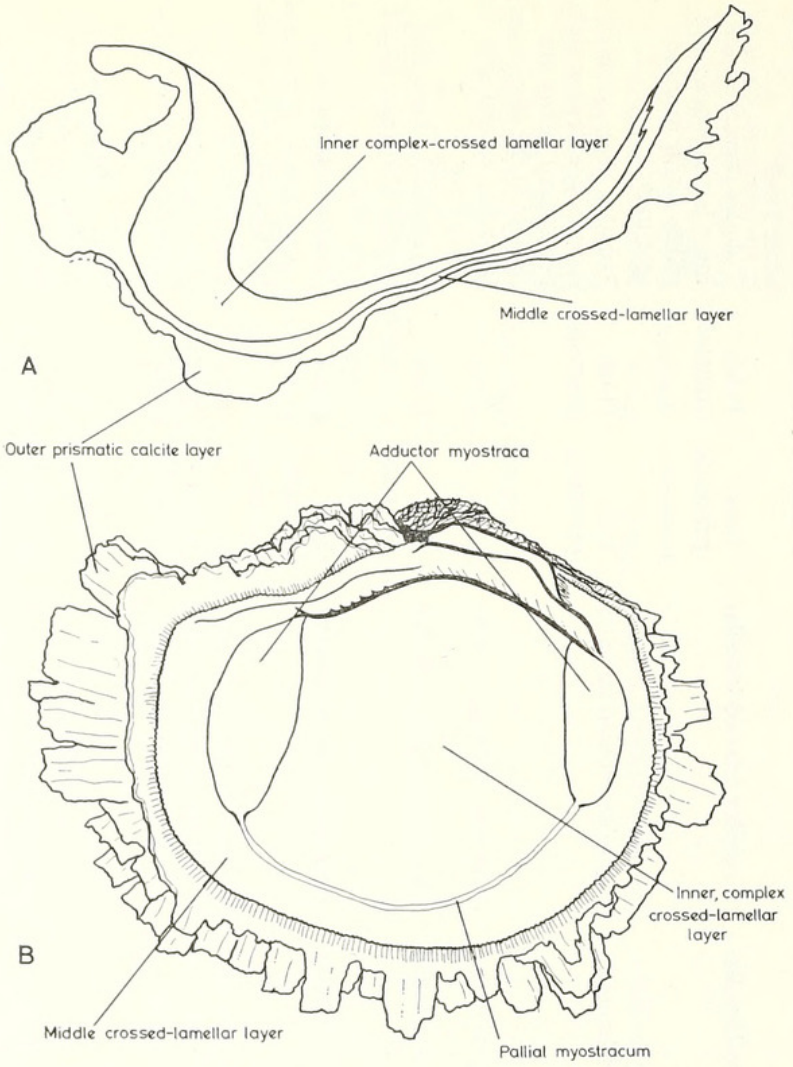

TEXT-FIG. 5. (A) Longitudinal section and (B) interior of *Chama pellucida* Broderip to show the distribution of shell layers.

EXPLANATION OF PLATE 73

All sections are acetate peels.

Fig. 1. Outer crossed-lamellar layer of *Arcinella arcinella* (Linnaeus), showing first-order lamels aligned normal to the shell interior in the inner part of the layer (lower), and the 'bladed' outer part where they are aligned parallel to the shell interior. Radial section, ×32.

Fig. 2. Radial section inner complex crossed-lamellar layer of *Chama calcarata* Deshayes showing cone shaped depressions in myostracal sheets, ×32.

Fig. 3. Planar section through the adductor myostracum of *Chama lazarus* Wood, ×100.

Fig. 4. Contact between the outer crossed-lamellar layer (left) and the adductor myostracum of *Chama radians* Lamarck, radial section, ×80.

Fig. 5. Myostracal pillars in the inner, complex crossed-lamellar layer of *Chama radians* Lamarck. Radial section, ×80.

Fig. 6. Radial section of the inner complex crossed-lamellar layer of *Chama lazarus* Wood, ×20.

Fig. 7. Myostracal sheets in the inner complex crossed-lamellar layer of *Chama lamellosa* Lamarck, ×80.

Fig. 8. Contact between the outer, prismatic, calcitic layer (top) and the middle aragonite crossed-lamellar layer of *Chama pellucida* Broderip, ×80.

Fig. 9. Planar section of the outer prismatic, calcitic layer of *Chama pellucida* Broderip, ×80.

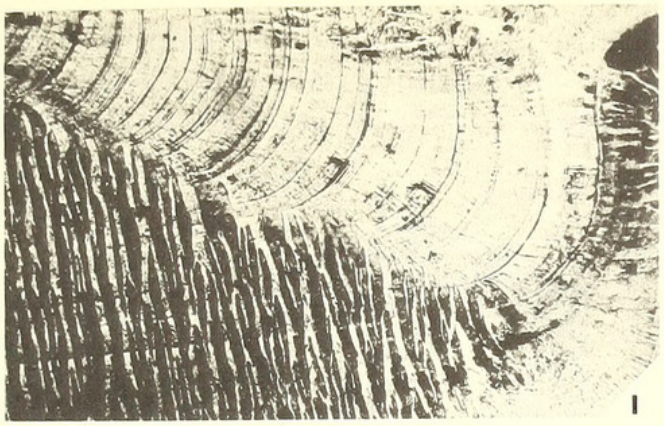

1

2

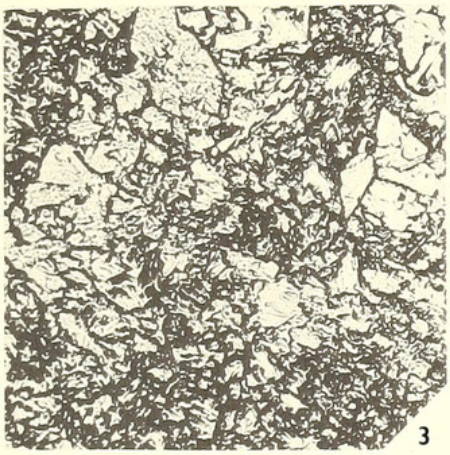

3

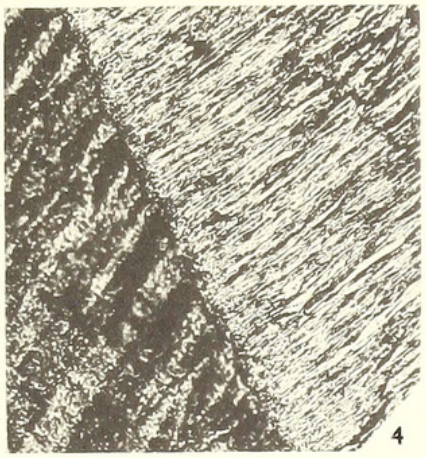

4

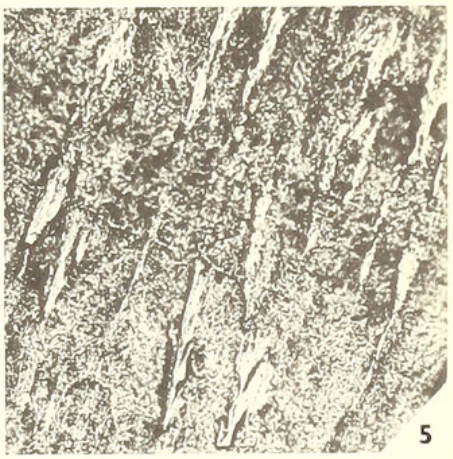

5

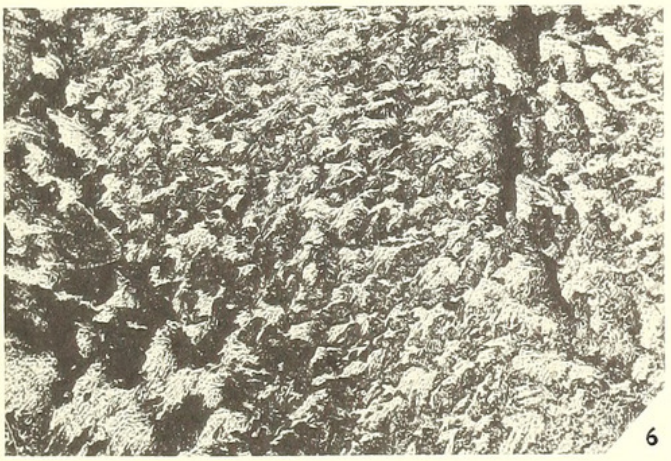

6

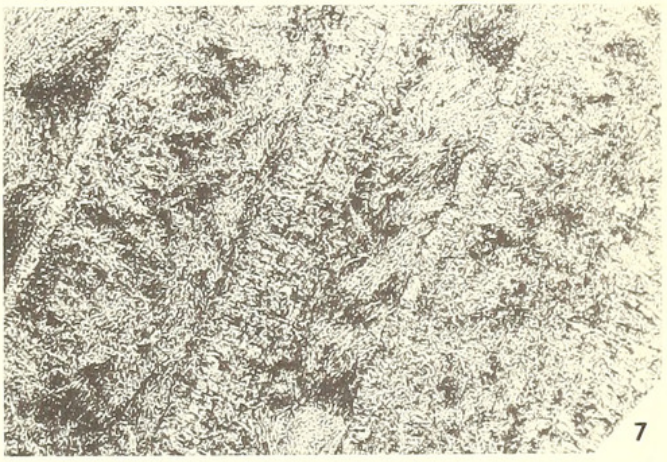

7

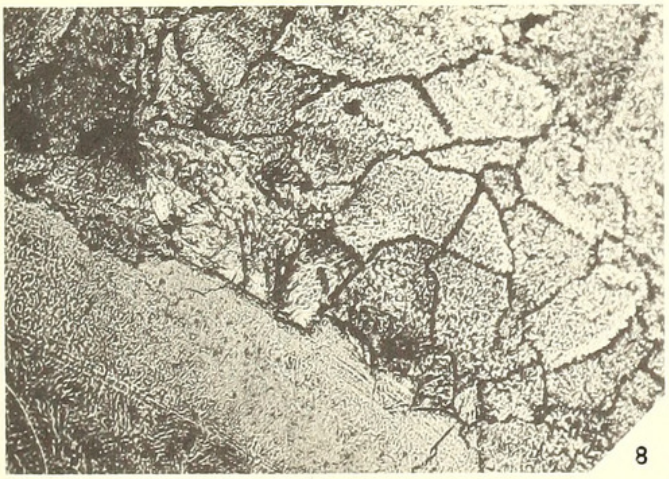

8

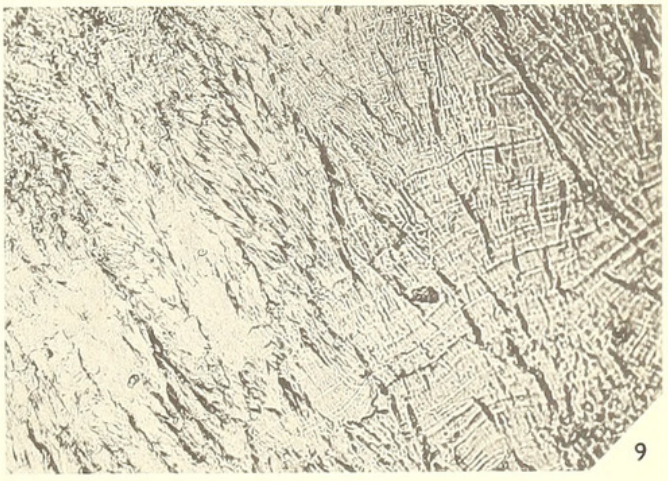

9

tens of microns long, joined in side-to-side contact. These sheets of laths, i.e. second-order lamels, lie normal to the sides of the first-order lamels, the long axes of the laths being parallel to the plane of the first-order lamels.

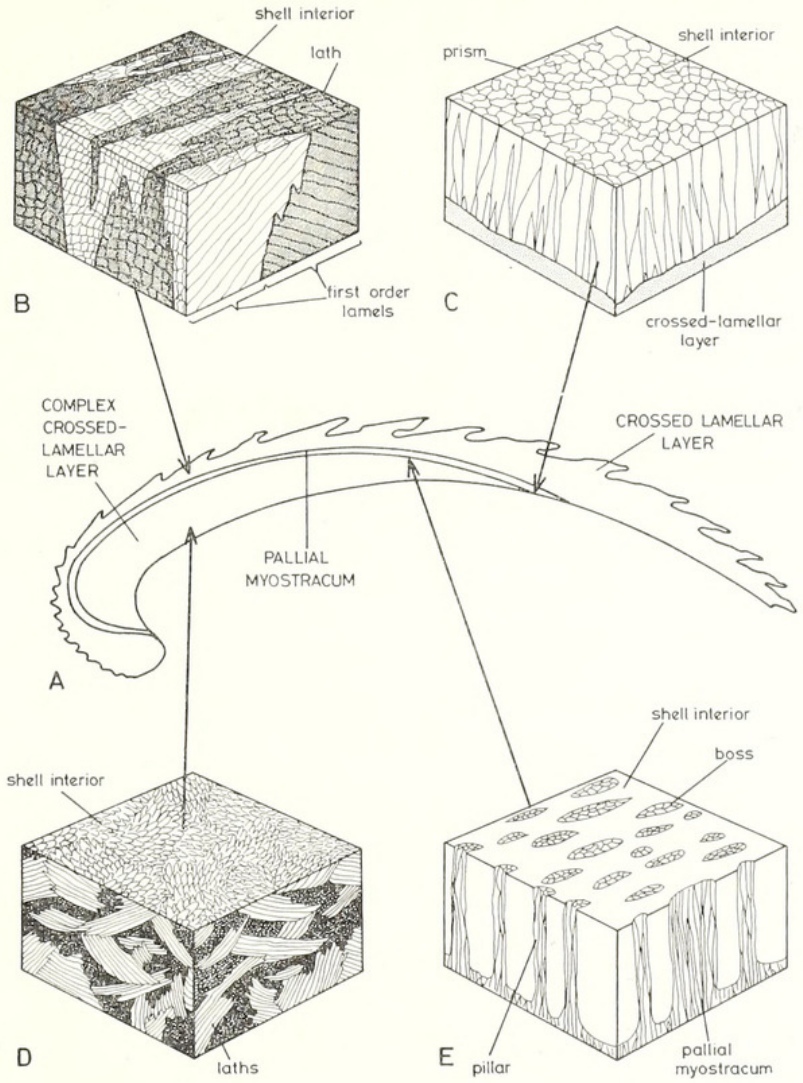

TEXT-FIG. 6. Radial section of a typical *Chama* (A) with block diagrams to show the microstructure of the crossed-lamellar layer (B), pallial myostracum (C), complex crossed-lamellar layer (D), and myostracal pillars (E).

Second-order lamels are inclined to the shell interior, with opposite inclinations of dip in adjacent first-order lamels. Optical work suggests that the whole layer is built of crystallites with only two crystallographic orientations.

These observations are summarized in text-fig. 6*b*. Fine structure is shown in Plate 74, fig. 1.

As well as the carbonate, there is a well-developed proteinaceous organic matrix in the crossed-lamellar layer (Pl. 74, fig. 2). This is intimately associated with the carbonate, surrounding each lath of the crossed-lamellar structure. Unlike the regular, fenestrate sheets of nacre organic matrix (Grégoire 1957, 1959, 1960, 1967), crossed-lamellar matrix has a much more open, irregular structure.

The variation in attitude of first-order lamels seen in sections is a result of their growth normal to the secreting surface, i.e. the marginal parts of the mantle. Where this is variable in form, as in ribs, or in the reflected margin of *Arcinella*, irregularities will develop. Indeed, in *Arcinella*, growth of lamels normal to the surface of the margin produces a structure which superficially resembles the composite prismatic structure developed in the Lucinacea (Pl. 73, fig. 1).

(*b*) *Structure of the complex crossed-lamellar layer.* Complex crossed-lamellar structure forms the inner shell layer of all Chamacea. We use 'complex crossed-lamellar' in the original sense of Bøggild (1930). It is thus equivalent to 'complex' structure of Oberling (1964), which is not to be confused with 'complex' of Bøggild (1930)!

This shell structure type is built of the same basic building blocks as crossed-lamellar structure, i.e. minute laths (Text fig. 6*d*). Instead of building first-order lamels, the laths build much more irregular blocks (Pl. 73, fig. 6; Pl. 74, fig. 3), and many different attitudes and orientations of laths are present within the layer.

In some sections, small irregular patches of radiating laths are recognizable. MacClintock (1967) has described these as sections of spherulitic growth. His patelloid structures are, however, different in detail from structures present in bivalves.

(*c*) *Structure of the prismatic layer.* An outer, calcite prismatic layer is present in two recent species of *Chama*, *C. pellucida*, and *C. exogyra*. The occurrence in *C. pellucida* has been noted by previous workers (Lowenstam 1954 *a*, *b*, 1963, 1964; Kennedy and Taylor 1968), but the present record from *C. exogyra* represents only the second occurrence of calcite in extant bivalves other than the Pteriomorpha.

However, matters are far from simple in respect of these two species.

Examination of the type specimens of *C. exogyra* and *C. pellucida* (in the collections of the British Museum (Natural History)) shows that the specimens appear distinctive. *C. pellucida* is rounded in outline, is 'normal' (i.e. attached by the left valve), and bears striking translucent squamae. *C. exogyra* is irregular, elongate, reversed (i.e. attached by right valve), and lacks conspicuous squamae. Other specimens of *C. exogyra* we have examined show rather more conspicuous ridges, and are 'normal'—attached by the left valve. These normal specimens closely resemble *C. pellucida*, whilst reversed *C. pellucida* closely resembles *C. exogyra*.

These similarities, the identical and highly unusual mineralogy and structure, together with the similar geographical range of the two species (Yonge 1967) plus the problems

---

EXPLANATION OF PLATE 74

All figures are scanning electron-micrographs.

Fig. 1. Polished, etched (HCl) radial section of the middle crossed-lamellar layer of *Chama pellucida*, showing three adjacent first-order lamels, ×700.

Fig. 2. As above, showing contact between the outer prismatic layer (left) and the middle crossed-lamellar layer; notice the lace-like organic matrix network, ×700.

Fig. 3. Fractured section of the inner complex crossed-lamellar layer of *Chama radians*, showing laths joined into second-order lamels having variable orientations, ×240.

Fig. 4. Inner shell surface of *Chama radians*, showing the outcrop of myostracal prisms, ×1,100.

Fig. 5. Polished, etched (HCl) radial section of the outer prismatic layer of *Chama pellucida*, ×700.

Fig. 6. Inner shell surface of *Chama radians* showing the opening of a tubule, ×2,250.

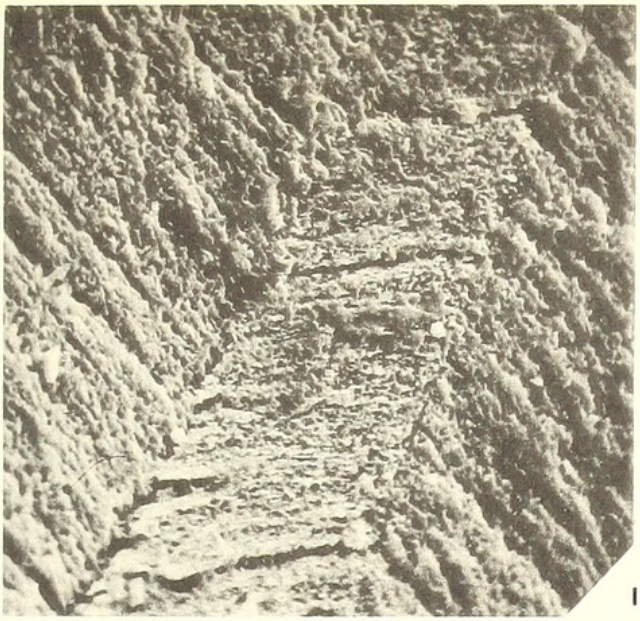
1

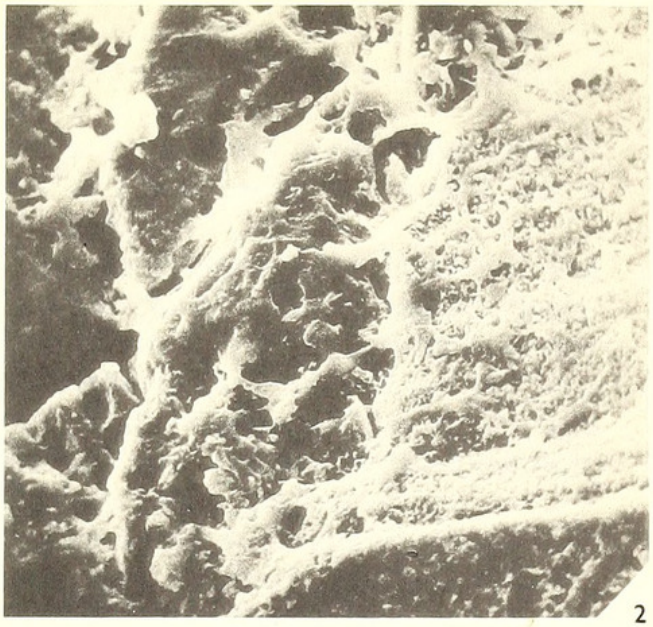
2

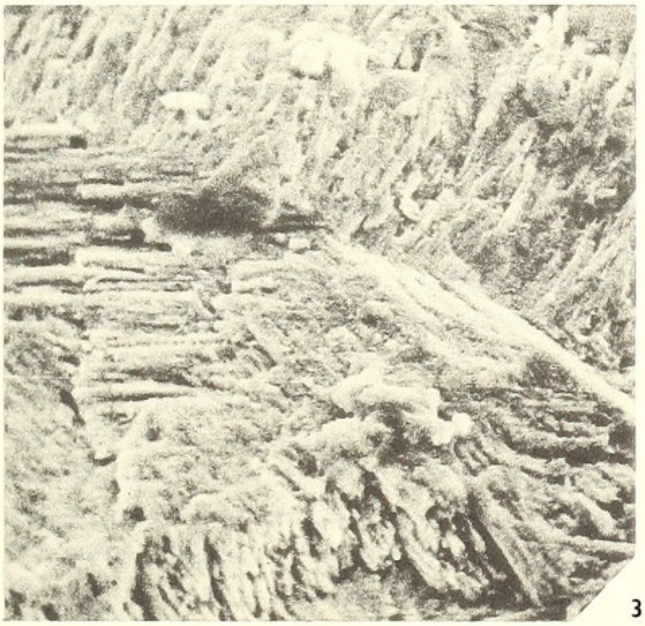
3

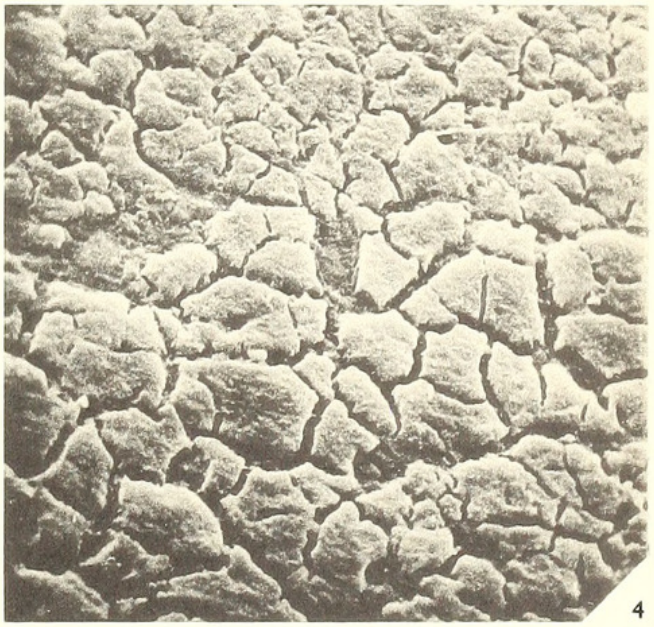
4

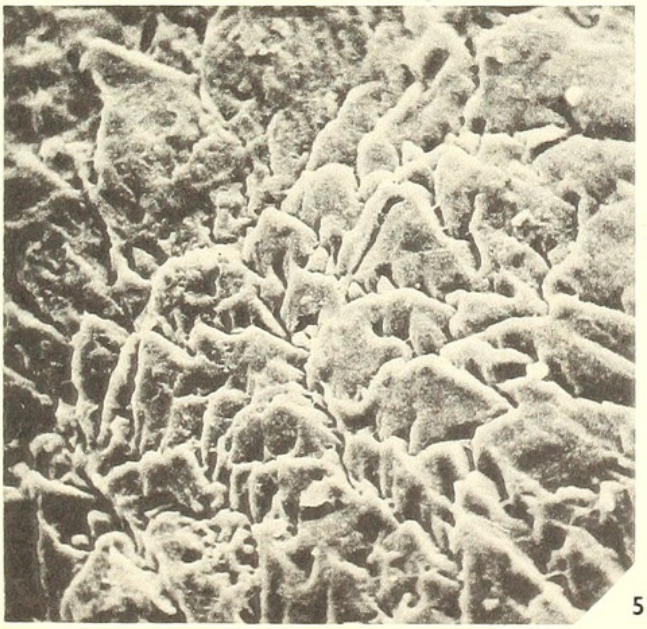
5

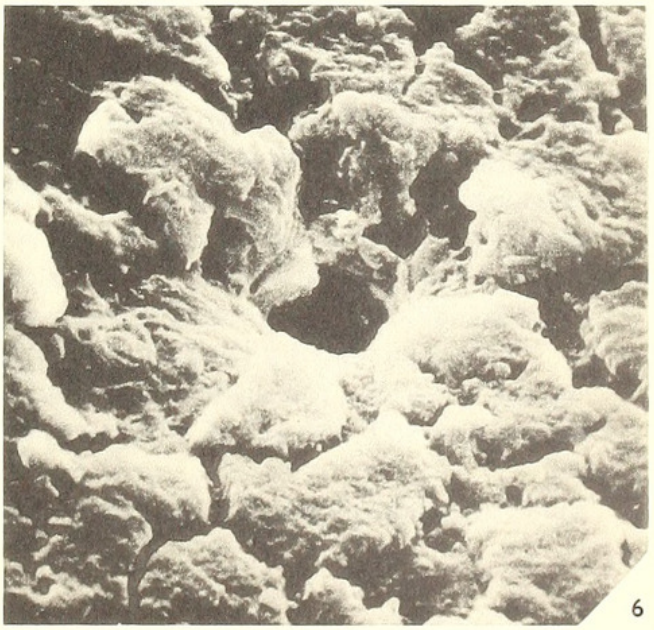
6

KENNEDY, MORRIS and TAYLOR, Chamacea

of inversion in the Chamacea generally, have led us to suspect that these species may be synonymous. This is, however, a field problem, which we cannot resolve on the basis of material available to us.

In both species the structure of the outer prismatic layer is very similar, and different from that occurring in all other extant bivalves. In hand specimen, the layer has a distinctive, translucent, 'pellucid' appearance (Pl. 70, fig. 3).

In peels and thin sections (Pl. 73, figs. 8 and 9) it appears grey against the browns and yellows of the adjacent crossed-lamellar layer. It is built up of minute, irregular, blade-like prisms, which are orientated more or less normally to the mantle and shell interior at the time of secretion. The prisms are rather variable in their attitude (in part as a result of their being involved in ribs and squamae), and are arranged into blocks with irregular polygonal outlines (Pl. 73, fig. 8). These larger blocks pass into extinction quite irregularly, and there is thus no uniformity of attitude within the blocks.

These observations are confirmed by electron-microscopy. In fractured sections, the large prism blocks show prominent transverse striae, and are clearly built up of smaller units (Pl. 77, fig. 2). Etching brings out these smaller units (Pl. 74, fig. 5), which correspond to the fine prisms seen at optical level. These fine prisms are surrounded by sheaths of organic matrix, but there are no thick conchiolin sheets such as characterize the other prismatic calcite layer of *Pinna*, *Pinctada*, and many other bivalves.

(*d*) *Structure of the myostracal layers*. These layers show similar features in all Chamacea we have examined. At optical level (Pl. 73, figs. 3, 4, 5, 7) myostraca are a characteristic grey colour, contrasting with the adjacent shell layers. The myostraca are built up of prisms, with highly irregular outlines. These prisms are orientated with their long axes normal to the surfaces of the myostracum, with crystallographic axes lying in the same direction (text-fig. 6*c*). There are no well-developed interprismatic protein walls, but thin organic matrix envelopes surround each prism.

The pallial myostracum is a thick sheet, extending into the umbo (text-fig. 6*a*). The adductor myostraca are thick, well-developed pads. In addition to these features, areas of myostracal structure are present in the Chamacea away from well-authenticated areas of muscle attachment. Sheets of myostracal-type prisms are present within the inner shell layer of many species, and represent interruption of deposition of normal shell fabric (Pl. 73, fig. 7). This may be due to periodic attachment of the mantle surface, but there is no direct evidence for this, although structure and fluorescence properties are identical with those of normal myostracum. Pillar-like areas of myostracal structure, called myostracal pillars (Taylor, Kennedy, and Hall 1969) occur in the inner layer of most species of Chamacea and in the crossed-lamellar layer of a few species (Table 1).

These pillars appear in sections as elongate ovoids or strips of myostracal structure, the long axes running normally to the shell interior (Pl. 73, fig. 5). In the inner layer they usually extend upwards from the pallial or adductor myostracum (text-fig. 6*e*).

On shell interiors, myostracal pillars outcrop as minute bosses, usually 0·5–1·0 mm. in diameter, or as elongate ovals, often arranged in lines radiating from the umbo.

Electron-microscopy shows that the surfaces of the bosses consists of a series of irregular prisms, corresponding to those seen at optical level (Pl. 74, fig. 4). The prisms are separated by grooves, of uncertain origin.

Sections of the mantle of *Chama jukesii* reveal the presence of minute papillae all over

the mantle surface, corresponding in size and distribution to the myostracal pillars of the shell. These papillae result from elongation of the normal mantle cells, and we take them to be sites of additional shell and mantle attachment.

A peculiar modification of the sheets of myostracal type prisms present in the inner shell layer is seen in *Chama calcarata* and *Chama gigas*. Here, the inner surface of the inner shell layer is pitted. These pits correspond to depressions in the surfaces of the myostracal sheets (Pl. 73, fig. 1), and presumably reflect another mode of shell/mantle attachment.

(*e*) *Layer contacts*. Crossed-lamellar and complex crossed-lamellar layers are separated by the pallial and adductor myostraca. There is usually a transition zone at the layer/myostracum contact, rich in organic matrix. The organic matrix of the myostracum and the crossed-lamellar or complex crossed-lamellar layers is in structural continuity. There is often a complex interdigitation of adductor myostracum and shell layers (text-fig. 4*a*). This is probably the result of slight shifting of the animal within its shell during growth.

The contact of the crossed-lamellar layer and the outer prismatic layer of *C. pellucida* and *C. exogyra* shows several unusual features (Pl. 73, fig. 8). The surface at contact is minutely corrugated, the corrugations apparently originating at the shell margin, as a reflection of the position of the pallial muscles. They are subsequently buried below the middle layer, filled by a thin zone of fine-grained aragonite, rich in organic matrix (Pl. 74, fig. 2). Elsewhere, this layer is replaced by a complex and irregular junction with minute angular crystals protruding into the crossed-lamellar layer, as though a highly irregular surface was grown over by crossed-lamellar structure. These relationships closely resemble the results of partial recrystallization of aragonite to calcite.

The organic matrix of prismatic and crossed-lamellar layers is in direct structural continuity.

(*f*) *Tubules*. Many species of Chamacea possess the remarkable shell feature which Oberling (1964) described as tubules (Pl. 74, fig. 8).

These are minute cylindrical perforations, only a few microns in diameter, which open at the interior surface of the shell and penetrate the shell layers. Tubules are a primary feature of the shell (Oberling 1964; Taylor, Kennedy, and Hall 1969), and appear as minute hollow cylinders penetrating the finest elements of the shell fabric (Pl. 74, fig. 8). On the shell interior, *Chama* tubules lie in minute pits. The function of tubules is at present unknown.

(*g*) *Ligament*. The ligament of the Chamacea is calcified and aragonitic, as in other bivalves with calcified ligaments (Lowenstam 1964; Taylor, Kennedy, and Hall 1969) (Pl. 77, fig. 1).

(*h*) *Banding*. All shell layers show prominent daily growth bands (Panella and MacClintock 1968).

COMPARISON OF THE CHAMACEA WITH OTHER GROUPS

The systematic position of the Chamacea has always been in doubt. Consideration of their affinities in the past was not helped by the allotment to this superfamily of several other cemented bivalves such as the rudists and the pandoraceans, *Cleidothaerus* and

Myochama. However, as it stands today, the superfamily Chamacea can be considered a homogeneous group.

The Chamacea have been related to the Lucinacea (Douvillé 1912, Nicol 1952), Carditacea (Dall 1903), the Cardiacea (Anthony 1905), Crassatellacea (Boehm 1891), Veneracea (Fischer 1886), and to the Hippuritacea (see references in Odhner 1919, Newell 1965, Yonge 1967). Of all these possibilities that of relationship to the rudists is the most commonly held. Odhner (1919) came to this conclusion after a detailed study of *Chama*, and Cox (1960) in deference to the thoroughness of Odhner's work accepted the conclusion but thought they should constitute a separate superfamily.

The similarities of the Chamacea to the various superfamilies listed above are discussed below. A summary of some of the more easily tabulated characters of possible relatives amongst living bivalve superfamilies is given in Table 2. The affinities with the extinct rudists are more difficult to examine because of the lack of soft parts, but Yonge (1967) has made certain inferences concerning rudist soft parts based on a study of the inner shell morphology.

1. *Comparison with the Carditacea*

Two distinct groups can be recognized within the Carditacea.
(*a*) The *Venericardia* group, which are burrowers with generally rounded shell outlines. The hinge plate is short and high, and the ornamentation usually consists of radial ribs.
(*b*) The *Cardita* group, consisting of byssate forms, ovoid to subrectangular in outline. The hinge plate is usually elongate and the anterior adductor muscle is somewhat reduced. The ornament is usually of radial ribs, but some species can produce squamae. This group contains many tropical species associated with coral reefs and rocky shores.

It is to this second group that the Chamacea may be compared. As can be seen from Table 2 some soft part characters such as the degree of mantle fusion and the gill plication are different, but others, such as labial palps and stomach types, are similar.

The greatest similarity between the Chamacea and the Carditacea is seen in shell characters such as the shell structure, dentition, ornament, and the similarity of the uncemented dissoconch of *Chama* to the adult byssate *Cardita*.

Thus the outer shell layer of the Carditacea consists of crossed-lamellar structure, with rather fine first-order lamels. The inner layer is built up of complex crossed-lamellar structure. Myostracal pillars are present in most species; in some the pillars are confined to the inner layer but in others they occur in both layers. Myostracal-type prisms can also be present, as fine sheets interbanded with complex crossed-lamellar structure in the inner layer. Tubules were present in all the species we have examined.

The dentition of the Carditidae shows striking similarities to that of the Chamacea. Both families have a 'lucinoid' dentition. The notation for *Cardita variegata* Bruguière, Recent, Seychelles is:

Right valve	n	0	1	0	1	0	1		
Posterior									Anterior
Left valve	n		0	1	0	1	0	1	
			D				d		